(25)

DR-1778-7

UCLA/PPG--985

DE86 012090

Tokamak Power Reactor Ignition and Time Dependent Fractional Power Operation

E.L. Vold, T.K. Mau and R.W. Conn

Fusion Engineering and Physics Program
Mechanical, Aerospace and
Nuclear Engineering Department
University of California, Los Angeles

UCLA-PPG-985 June, 1986

Submitted to Fusion Technology

Tokamak Power Reactor Ignition and Time Dependent Fractional Power Operation

Table of Contents

Abstract 1

1. Introduction 3

2. Calculational Model 4

2.a. Basic Equations and Solution Methods 5

2.b. Power Terms 8

2.b.1. Alpha Thermalization 8
2.b.2. Auxiliary Power 10
2.b.2.i. Simple RF Model 10
2.b.2.ii. Feedback Auxiliary Power Model 10
2.b.3. Transport Power Loss 11
2.b.3.i. Conduction and Convection 11
2.b.3.ii. Ripple Loss 13
2.b.4. Radiation 13
2.b.5. Ohmic Heating 14
2.b.6. Rethermalization 15

2.c. Beta Limit 15

2.d. Density Limit 16

2.e. Energy Confinement Time 17

3. Discussion of Results 20

3.a. Confinement Uncertainties 20

3.b. Steady State Analysis 22

3.b.1. Ignition Contours 22
3.b.1.i. Confinement Degradation with Alpha Power (Compact Versus INTOR Size Tokamaks) 23
3.b.1.ii. Weak Confinement Degradation with Alpha Power 27
3.b.1.iii. Ignition Sensitivity to Ratio of Ion to Electron Confinement 29
3.b.1.iv. Ignition and Auxiliary Power 30
3.b.2. Reactor Parameters in (n-T) Space 32
3.b.2.i. Ignited Operating Restrictions 33
3.b.3. Thermal Control by Impurity Radiation 34
3.b.4. Thermal Control by Divertor Mode Operation 35

4. Time Dependent Histories 36

4.a. Soft beta Limit 37

4.b. Active Feedback for Thermal Stability in the Low Density, Higher Temperature Region 39

4.c. Active Feedback for Thermal Stability in the High Density, Low Temperature Region 41

4.d. Confinement Degraded with Temperature 43

5. Fractional Power Operation Scenarios 45

5.a. Confinement and Auxiliary Power 46

5.b. Temperature Dependent Confinement 47

5.c. Optimum Ignition Conditions 48

6. Discussion and Conclusions 51

References 55

Tables 58

List of Figures and Figure Captions 60

Figures 63

Tokamak Power Reactor Ignition and Time Dependent Fractional Power Operation

Abstract

A flexible time-dependent and zero-dimensional plasma burn code with radial profiles was developed and employed to study the fractional power operation and the thermal burn control options for an INTOR-sized tokamak reactor. The code includes alpha thermalization and a time-dependent transport loss which can be represented by any one of several currently popular scaling laws for energy confinement time.

Ignition parameters were found to vary widely in density-temperature (n-T) space for the range of scaling laws examined. Critical ignition issues were found to include the extent of confinement time degradation by alpha heating, the ratio of ion to electron transport power loss, and effect of auxiliary heating on confinement. Ignition will probably not occur in an INTOR tokamak if all of the alpha power degrades confinement. Applied to a compact tokamak, ignition would be marginally likely. If only the auxiliary heating degrades confinement, the ignited operating region shows the interesting characteristic of the plasma temperature increasing in response to a decrease in auxiliary power due to the resulting greater decrease in transport losses. If ion confinement is neoclassical (τ_i/τ_e large), the ignition criteria are much more optimistic than for anomalous ion loss, even when the total transport loss is governed by a specific scaling law.

Feedback control of the auxiliary power and ion fuel sources are shown to provide thermal stability near the ignition curve. A potential problem will arise if the ignition curve falls below the regions of (n-T) space where the desired reactor net electric power results. Then, net output power occurs in a thermally unstable region. Mechanisms to stabilize this region are

investigated including a "soft-beta" limit, auxiliary feedback, impurity radiation, divertor mode variation, varying ion to electron confinement times, and various means of increasing transport power losses. Only the "soft" beta limit is unambiguously stabilizing, although confinement degradation by a small fraction (~15%) of the alpha power would also provide passive thermal stability. Confinement degraded proportionally to plasma temperature, rather than to input power, is shown to marginally provide thermal stability near the ignition curve. In the case of confinement time degraded by auxiliary heating, thermal stability in operating regions well above the ignition curve can be maintained by active feedback of the auxiliary power systems, but very reliable feedback control will be required to avoid thermal runaway.

We conclude that thermal control and fractional power operation of a tokamak reactor with ignited plasma is far from a trivial problem. Several possible approaches have been suggested for thermally stable operation in the ignited regime. If ignition is not achieved, thermal stability is achieved in a driven sub-ignited reactor mode. These approaches must be evaluated further and with more refined empirical estimates for the energy confinement scaling in order to reduce the present uncertainty in this area.

Time Dependent Plasma Thermal Analysis

1. Introduction

The eventual utilization of the tokamak fusion reactor as a commercial power source necessitates a thorough understanding of the operational requirements at full and fractional power levels. In this study, we examine the dynamics involved in the startup and heating of the tokamak reactor to its full power level via intermediate power plateaus. In particular, we study the role of burn control in maintaining the plasma at thermal equilibrium throughout these operations. More importantly, methods to control the reactor output power and to transit between intermediate fractional power stages are identified.

The analytical tool consists of a zero-dimensional, time-dependent plasma power balance model with fixed density and temperature profiles. Because the plasma power balance is dominated by the transport loss and given the large uncertainty in the confinement model, we have studied the problem for a wide range of energy confinement scalings, discussed further in Sec. 2.e. These scalings for global confinement time τ are most often empirical and can be divided into three groups: (A) τ independent of heating power, (B) τ degraded with auxiliary power, and (C) τ degraded with both auxiliary and alpha power. As such, a detailed comparison of ignition criteria for those scaling laws was also carried out with the use of steady-state analysis. The results of this analysis form the basis for studying the temporal behavior of the plasma under various thermal control mechanisms. Scenarios of thermally stable full and fractional power operations have been determined for a variety of transport models, with either passive or active feedback burn control.

Important power control parameters, such as gas fueling rate, auxiliary power and other plasma quantities that affect transport losses, have also been identified. The results of these studies vary with the individual transport scaling used and, in particular, with respect to the effect of alpha heating power on confinement.

The contents are outlined as follows. Section 2 gives a description of the calculational model and techniques used in this study. This is followed by Sec. 3 in which results of the steady-state analysis are presented. Section 4 gives the results of time-dependent analyses for various thermal control scenarios under a wide range of operation conditions. In Sec. 5, scenarios of fractional power operation are explored. Discussion of results and a list of conclusions are given in Sec. 6.

2. *Calculational Model*

The main features of the calculational model are given here and described in greater detail in the following sections.

1. Time-dependent analysis solves five coupled nonlinear ordinary differential equations for the time evolution of ion density, alpha density, ion and electron temperature, and an average alpha temperature. Electron density is determined from charge neutrality.

2. Plasma power balance terms are integrated over parabolic radial profiles with variable exponential and edge fractions.

3. Confinement scaling laws based on experimental results are used to determine energy transport losses which are partitioned between the ions and the electrons.

4. Alpha thermalization is included via a numerical evaluation of the classical Coulomb energy loss to a Maxwellian background, while tracking the

alpha energy groups during slowing down.

5. Transport loss may be changed with a response time characteristic of the energy confinement time or, optionally, of the heating power thermalization time.

6. Feedback to auxiliary power can be used to linearly ramp the temperature in time at a constant density. By successively incrementing density and sweeping the temperature at constant density, the reactor operating parameter contours in density-temperature (n-T) space are generated. For a sufficiently small temperature ramp rate, these contours approximate 'equilibrium' parameter values.

7. This study focused on an INTOR-size tokamak as part of the UCLA project on Fractional Power Operation of a Tokamak Reactor. The basic device parameter values are given under "INTOR/UCLA" in Table I. The table also includes values for two compact ignition tokamaks, which are discussed further and included only in the ignition analysis section.

2.a. Basic Equations and Solution Method

The set of equations for the time dependent analyses include the particle conservation equations for the mean fuel ion density n_i and for alphas, n_α and energy conservation equations for mean particle energies, T_i, T_e, T_α for ions, electrons, and alphas, respectively. Electron density is obtained by assuming charge neutrality. The system of equations is written in the form:

$$\frac{\partial n_i}{\partial t} = \left(S_i - \left[\int n_i^2 f_D(1 - f_D)\langle\sigma v\rangle\, dr\right] - \frac{n_i V_p}{\tau_{pi}}\right)/V_p \qquad (1)$$

$$\frac{\partial n_\alpha}{\partial t} = \left(\left[\int n_i^2 f_D(1 - f_D)\langle\sigma v\rangle\, dr\right] - \frac{n_\alpha V_p}{\tau_{p\alpha}}\right)/V_p \qquad (2)$$

$$\frac{\partial T_i}{\partial t} = \left(\frac{\Sigma P_i}{1.5 V_p} - T_i \frac{\partial n_i}{\partial t}\right)/n_i \qquad (3)$$

$$\frac{\partial T_e}{\partial t} = \left[\frac{\Sigma P_e}{1.5 V_p} - T_e \frac{\partial n_e}{\partial t}\right]/n_e \tag{4}$$

$$\frac{\partial T_\alpha}{\partial t} = \left[\frac{\Sigma P_\alpha}{1.5 V_p} - T_\alpha \frac{\partial n_\alpha}{\partial t}\right]/n_\alpha \tag{5}$$

where: $n_e = n_i + 2 \quad n_\alpha$ (6)

$$\frac{\partial n_e}{\partial t} = \frac{\partial n_i}{\partial t} + 2 \quad \frac{\partial n_\alpha}{\partial t} \tag{7}$$

S_i = volume integrated ion fuel source

$\int(\ )\ dr$ = plasma volume integral

V_p = total plasma volume

τ_{pj} = particle confinement time for species j

ΣP_j = sum of the volume integrated power terms for species j:

The power terms considered in this model include:

$$\Sigma P_i = P_{\alpha i} + P_{aux,i} + P_{ie} - P_{tr,i} \tag{8}$$

$$\Sigma P_e = P_{\alpha e} + P_{aux,e} - P_{ie} - P_{tr,e} + P_{oh} - P_{rad} \tag{9}$$

$$\Sigma P_\alpha = P_{fus} - P_{\alpha i} - P_{\alpha e} \tag{10}$$

Each of these terms are volume integrals (MW total), where:

$P_{\alpha j}$ = alpha thermalization power to species, j

$P_{aux,j}$ = auxiliary power to species, j

P_{ie} = ion-electron rethermalization

$P_{tr,j}$ = total transport loss (including energy conduction and convection) for species, j

P_{oh} = ohmic heating power

P_{rad} = total radiation loss including bremstrahlung and synchrotron radiation

P_{fus} = alpha power released in fusion

The radial (r) profiles for the density and temperature of each species, j, are computed in the form:

$$n_j(r) = n_{jo}(1 - (1 - f_j)r^2/a^2)^{pf_j} \qquad (11)$$

where:

n_{jo} = the peak value of density (or temperature) for species j

f_j = the fraction of the peak value at the plasma edge (= 0.02)

pf_j = the profile factor

a = plasma minor radius

The power terms [in Eqs. (8), (9) (10)] are integrated over the plasma volume using the profiles [in Eq. (11)] expressed in the general form:

$$P(MW) = 4\pi^2 R_o K C_k \int_0^a p(W/m^3)\, r\, dr \qquad (12)$$

where:

R_o = major radius

K = plasma elongation

C_k = energy conversion factor for the power term, k

$p(w/m^3)$ = power density as a function of radius, r

The density can be fixed during a time-dependent run and the required ion-fuel source is computed. Multiple time dependent sweeps ramping up the temperature at constant density can be combined while successively incrementing the density for each sweep. Operating parameters can then be plotted in the resulting density-temperature space as in the POPCON plots generated by the ORNL Tokamak Code, WHIST.[1] For a sufficiently small temperature ramp rate, these results approach the equilibrium values ($dT/dt \cong 0$), and the resulting "pseudo-equilibrium" contours give valuable information on reactor steady-state operation.

2.b. Power Terms

2.b.1. Alpha Thermalization

For simplicity, alpha thermalization can be assumed to be instantaneous, and thus, Eq. (5) can be dropped from the system of equations. $P_{\alpha i}$ and $P_{\alpha e}$ [in Eqs. (8) and (9)] are replaced by ($f_{\alpha j}$ P_{fus}) where $f_{\alpha j}$ is the fraction of alpha power going to species, j, at the present plasma conditions. Instantaneous alpha thermalization is a good approximation under steady-state conditions. Since it is extremely fast computationally, this assumption is used in some cases, for instance, in generating the pseudo-equilibrium contour plots. For a more exact treatment by the code, the alpha thermalization terms are retained explicitly in Eqs. (8), (9), (10) as $P_{\alpha i}$ and $P_{\alpha e}$. These are computed by numerical integration over all alpha energies and their sources contributing to the thermalization power in the current integration time interval, as described by the equation

$$p_{\alpha j}(W/m^3) = c_{\alpha j} \int_{t_i}^{t_{i+1}} S_\alpha(t') \frac{dW_{\alpha j}(t)}{dt} dt \qquad (13)$$

where $c_{\alpha j}$ = energy conversion factor

S_α = alpha source density (m-3 s-1) at time, t', which contributes to thermalization energy in the current time interval from t_i to t_{i+1}.

$\frac{dW_{\alpha j}}{dt}$ = energy loss rate (KeV s^{-1}) from alpha particle at time, t, to species, j.

The energy loss rate for the alpha particle slowing down in a Maxwellian plasma of species, j, is given by:

$$\frac{dW_{\alpha j}}{dt} = \frac{-n_j e^4 Z_j^2 \ln\Lambda}{4\pi\varepsilon_o^2 m_j v_j} H(V_\alpha/V_j,\ m_j/m_\alpha) \qquad (14)$$

where $v_j = (2T_j/m_j)^{0.5}$ = thermal velocity of species j, with mass, m_j, and energy, T_j.

e = electron charge

$\ln\Lambda$ = coulomb logarithm for species j

ε_o = permitivitty of free space

n_j = density of species j

Z_j = atomic charge of species j

and:

$$H(x,\ m_j/m_\alpha) = \text{erf}\ (x)/x - (2\pi)^{-0.5}(1. + m_j/m_\alpha)\ \exp(-x^2)$$

where $x = V_\alpha/V_j = (M_j W_\alpha/M_\alpha T_j)^{0.5}$

2.b.2. Auxiliary Power

2.b.2.i. Simple RF Model. The fixed profiles given by Eq. (11) do not easily lend themselves to an accurate accounting of RF absorption. It was assumed that over the range of plasma parameters examined, the auxiliary RF power has a constant fraction going to the ions (usually 0.8) and a constant net absorption efficiency, defined as power absorbed by the plasma per unit of power delivered to the RF generator (usually set at 0.55). These assumptions are sufficiently accurate for the present purposes of examining global power balances.

The RF power can be fixed at a constant level, or varied with a programmed time dependence, or it can include the feedback scheme discussed below.

2.b.2.ii. Feedback Auxiliary Power. The constant temperature ramp rate is fixed by the linear feedback scheme with feedback power, P_{fdbk}, based on the equation:

$$P_{fdbk} = -P_{net} + P_{ramp} + \frac{E}{\tau_{efn}} - \frac{(E - E_{ramp})}{\tau_{fdbk}} \qquad (15)$$

where $P_{net} \sim P_{fus} + P_{oh} - P_{rad}$

P_{ramp} = power required for desired temperature ramp rate

= $(k_r \bar{n} V_p)$ and k_r is the desired ramp rate input

E = actual plasma energy present.

= $3\bar{n}\bar{T}V_p$ for: $\bar{n} = (\bar{n}_e + \bar{n}_i)/2$

$\bar{T} = (\bar{T}_e + \bar{T}_i)/2$

E_{ramp} = present plasma energy for desired ramp rate

= $(P_{ramp}\ t)$ for t = current time

τ_{cfn} = global confinement time

$= 3\overline{nT}/P_{tr}$

τ_{fdbk} = feedback scheme response time (fixed input, default = 0.4 sec)

2.b.3. Plasma Transport Power Loss

2.b.3.i. Conduction and Convection. The transport power loss contains the largest uncertainty in the plasma power balance due to uncertainty in the energy and particle confinement scaling laws. This is especially true when the results of derived scaling laws are extrapolated to the regime of an ignited power reactor. As such, our calculational model has allowed for a range of scaling laws and simple relations between ion and electron scalings and between particle and energy confinement in order to easily interpret the differences in results between the scaling laws examined here. Since the scaling laws are often in the form of an empirical relation involving global plasma paramters, this code utilizes global averages of density and temperature when computing specific confinement times.

We assume that total transport loss, P_{tr}, can be written for electrons, e, and for an average fuel ion species, i, simplified for global averages as:

$$P_{tr} = \frac{3}{2}\frac{\bar{n}_e\bar{T}_e}{\tau_{pe}} + \frac{3}{2}\frac{\bar{n}_e\bar{T}_e}{\tau_{Ee}} + \frac{3}{2}\frac{\bar{n}_i\bar{T}_i}{\tau_i} + \frac{3}{2}\frac{\bar{n}_i\bar{T}_i}{\tau_{Ei}} \qquad (16)$$

Each of these confinement times can be simply related to a given experimentally (or theoretically) determined confinement time from a global scaling law, τ_{gs}, which is generally evaluated from the equation:

$$P_{tr} \sim P_{INJECTION} = \frac{3\,\bar{n}\,\bar{T}}{\tau_{gs}} \qquad (17)$$

For the typical case where $n_e \sim n_i$ and $T_e \sim T_i$, comparing Eqs. (16) and

(17), the following relation must hold:

$$\frac{1}{\tau_{gs}} = \frac{1}{2}\left(\frac{1}{\tau_{pe}} + \frac{1}{\tau_{Ee}} + \frac{1}{\tau_{pi}} + \frac{1}{\tau_{Ei}}\right) = \frac{1}{2\tau_{Eff}} \tag{18}$$

which says that the global confinement time, τ_{gs}, will be twice the effective confinement time, τ_{Eff}. Thus, one can vary each of the confinement times in Eq. (16) as a fraction of the global confinement, such that Eq. (18) is satisfied, and while simultaneously, the experimentally determined constraints regarding the relative magnitude of τ_{pi}, τ_{pe}, τ_{Ei}, and τ_{Ee} are satisfied. Since these relative magnitudes are only roughly known from experiments and there is considerable uncertainty here, we selected the following relations as appropriate to test the relative merits of the confinement scaling laws examined in this study.

We let $\tau_{gs} = \tau_{Ee}$ since the electron energy transport is considered the major transport loss channel. Some experiments indicate that energy loss times tend to be 10-100% of particle loss times, and we allow electron and ion particle loss rates to be similar. We have taken $\tau_{pi} \sim \tau_{pe} \sim 5\tau_{gs}$. As the τ_p values increase, the fuel source required at a given operating point decreases. In order to satisfy Eq. (18), we must then let $\tau_{Ei} \sim 1.67\tau_{gs}$ for the above values of τ_{Ee}, τ_{pi} and τ_{pe}. In this case, the ion energy loss is nearly as large as the electron energy, which corresponds to an anomalous ion energy loss. This is consistent with recent experimental observations on Doublet-III.[6] If we had selected τ_{Ee} to be smaller, i.e., less than τ_{gs}, then τ_{Ei} could be relatively larger corresponding to smaller (neoclassical) ion energy losses. In this model these differences become important, as discussed in Sec. 3. In summary then, the net transport loss follows Eq. (17) for each scaling law and also Eq. (18) is satisfied for the

partitioning of confinement between ions and electrons. The various scaling laws used for τ_{gs} are discussed separately in a following section.

2.b.3.ii. Ripple Loss. Early studies showed that the ion energy transport power loss due to ions trapped in the ripples of the toroidal magnetic field, and to the banana trapped ions, has a strong temperature dependence.[7] More recently, the ion ripple loss has been found to exhibit the $T^{3/2}$ dependence only up to about 5 keV and to roll off and even decrease above that temperature.[8] Thus, in the reactor operating temperature range the net ripple transport losses are likely to be orders of magnitude less than previously predicted and so, much less than the anomalous energy confinement losses. For this reason, ripple loss was omitted from our time dependent model. However, since ripple loss varies as $\delta^{9/2}$, where δ is the percent of field ripple, it may still be useful as an active thermal control mechanism, in which some of the saddle coil currents can be varied to induce larger ripple loss.[8]

2.b.4. Radiation

Radiation power loss is integrated over the plasma profile using Eq. (12) where:

$$P_{rad} \approx P_{brem} + P_{sync} \tag{19}$$

and

$$P_{brem} = 4.8 \times 10^{-43} \cdot n_e(r) n_i(r) Z_{eff} \cdot T_e^{0.5} \tag{20a}$$

$$P_{sync} = 6.2 \times 10^{-23} \cdot B \cdot r^2 \cdot K \cdot R_F \cdot n_e(r) T_e(r) \left(1. + \frac{T_e(r)}{146} + \ldots\right) \tag{20b}$$

where the synchrotron radiation parameters include:

$$K = \text{plasma absorption coefficient}$$
$$= 5 \times 10^{-3} \quad T_e(r)^{1.5}/(6.025e\text{-}17 \quad n_e(r) \quad a/B_r)^{0.5} \qquad (21)$$

and:

$$R_f = (1 - R)^{0.5} = 0.22 \text{ (for reflectivity, } R = 0.95)$$

2.b.5. Ohmic Heating

Ohmic heating power density is taken to be:

$$p_{oh}(MW/m^3) = 1. \times 10^{-6} \eta j^2 \qquad (22)$$

The parallel resistivity, η, for a tokamak is calculated from the Spitzer resistivity, η_{sp}:

$$\eta_{sp} = 2.4 \times 10^{-9} \quad Z_{eff}^{\ 2} \ln A_e/T_e^{\ 1.5} \quad , \qquad (23)$$

and using the neoclassical correction factor:

$$\eta = \eta_{sp}/(1 - 1.95(a/R_o) + 0.95 \quad (a/R_o)) \qquad (24)$$

Since ohmic drive to ignition is not a subject of this study we used the simplest method appropriate to this scoping model. To evaluate the total ohmic heating power, Eq. (23) for resistivity is evaluated at the plasma averaged temperature and density, and the average current density is used in evaluating the ohmic heating power density [Eq. (22)].

2.b.6. Rethermalization

Electron-ion power exchange or rethermalization power is integrated using Eq. (12), where:

$$p_{ie}(MW/m^3) = \frac{3}{2} \frac{(n_e(r)T_e(r) - n_i(r)T_i(r)}{\tau_{ie}} \tag{25}$$

and $$\tau_{ie} = 1.0 \times 10^{19} \quad (M_j \; / \; M_{proton}) \quad T^{3/2}/(n \; \ln\Lambda) \tag{26}$$

for S.I. units, except T(r) in KeV.

2.c. Beta Limit

The dependence of the beta limit on reactor device and operating parameters is important in two respects. First, the reactor operating parameters required to maximize the beta limit must be known to achieve maximum power operation. Second, if the beta limit turns out to be soft, thermally stable operation at the beta limit may be possible. In that case, burn control may be implemented by varying the beta limit through its dependence on operating parameters.

Similar scaling laws have been derived by at least three authors[11] for the MHD-stable beta limit β_c and its parameter dependence is given by:

$$\beta_c \; (\%) = \frac{c \; I_p(MA)}{a(m) \; B_T(T)} \tag{27}$$

where c = 1.8 - 4.4. Setting c = 3.3, gives the value defining the "Troyon beta limit".[12] The reactor parameter values from the present study (from Table I) give: $\beta_c(\%)$ = 3.3%(.97) ~ 3.2%.

A tokamak plasma geometric dependence of the beta limit has been worked

out by C. Bernard[13] in the useful form:

$$\beta(\%) \leq 27 \quad \varepsilon^{1.3} K^{1.2} (1 + 1.5\delta)\, q^{-1.1} \tag{28}$$

In the present study, these values become:

$\varepsilon = a/R_o = 1.2/5.3 = .226$

K = elongation = 1.6

δ = triangularity = 0.3

q = safety factor = 2.1

and we obtain a limiting beta value of 4.4%. For this study, we have assumed an intermediate value of 3.5% as the base case beta limit.

If Eq. (28) could be extrapolated to reasonable limits for δ and q, we would find a maximum beta of 5.3% as $\delta \to 0.5$. If we could simultaneously extrapolate while pushing $q \to 1.8$ we get beta ~ 6.3%. Further, if we let $a \to 1.4$, then $\varepsilon = 0.264$ and $\beta_{max} \sim 7.7\%$. While these extrapolations look optimistic, they are no longer necessarily consistent with Eq. (27) or with the maximum theoretical beta limits expected in the first stability regime.

2.d. Density Limits

The maximum stable operating density should be *consistent with the Murakami density limit for MHD stability.*[14] *This density limit,* n_{max}, is given by:

$$n_{max}(10^{20} m^3) = k_m \frac{B_o}{qR} \tag{29}$$

where: $k_m \sim 1.5$ for ohmic heated discharges,

~ 2-3 for auxiliary heated plasmas.

For the INTOR device used throughout most of this study, this sets a

density limit of about $1.5 \times 10^{20} m^{-3}$. This value, as we shall see, is probably not restrictive due to the greater limitation imposed by thermal stability requirements.

2.e. Energy Confinement Time

The scaling laws for energy confinement time that were examined in this study are shown in Table II. For some time, the INTOR/Alcator scaling law was considered somewhat of a standard, having been used in several tokamak design studies including INTOR in its earlier design stages.[8] Recently, a consensus has been reached that confinement time degrades with increasing auxiliary power added to the plasma. The empirical scaling has been determined from experimental data fits by Kaye and Goldston[15] for several tokamaks, and confirmed for the JET tokamak.[16] Thus, the scaling has been revised for INTOR[11] to one more consistent with the recent experimental findings that show decreasing confinement time with increasing plasma temperature or with increasing auxiliary heating power.

An early confinement scaling which accounted for this confinement degradation with plasma energy by including a $T^{\sim 0.5}$ factor is the Mereshkin scaling.[17] It shows a strong major radius dependence, R^3, which scales well with the large INTOR-sized tokamak, resulting in very optimistic performance predictions (discussed further in the following section).

The Goldston,[18] Ohkawa[19] and Kaye-Goldston[15] scalings are representative of the recently derived scaling laws which account for confinement degradation with auxiliary heating, P_{aux}, or total heating, P_{IN}.

In Goldston's work[18] and independently by Ohkawa,[19] an exponential fit for the form of confinement scaling could be written as:

$$\tau_E \quad P_{HEAT}^{-0.5}$$

where P_{HEAT} is a total heating power added to the plasma. The Goldston empirical law combines in inverse quadratic form, two terms which represent the two confinement regimes observed when, one, ohmic heating dominates and two, when auxiliary heating dominates.

Goldston combines two separate τ_E terms representing the ohmic and the auxiliary heating effects on confinement time, then at ignition, the ohmic term can be considered small, and so its density dependence can be neglected. This inverse quadratic combination of Goldston's τ_E was recently reviewed[20] and found to be consistent with the most recent experimental data from NBI and RF heated tokamaks which reflected a saturation of confinement time with increasing density. Alternatively, Ohkawa formualtes the auxiliary heating as a correction factor to the ohmic confinement; thus, the density dependence is retained even when the auxiliary (or alpha power) dominates over the ohmic power.

Ohkawa's theory-based scaling law similarly includes these two terms for auxiliary and for ohmic heating; however, here the terms are not separate. The auxiliary heating acts to decrease the basic confinement scaling which is neoalcator ($\sim n\, a\, R^2$) and proportional to q and to $T^{-0.5}$. Since Ohkawa's law degrades confinement for both auxiliary power ($P_{aux}^{-0.5}$) and for plasma energy density ($T^{-0.5}$), it is more pessimistic than the other scaling laws in terms of achieving ignition.

The Kaye-Goldston formula is an empirical regression analysis result, where they have opted to use injected power as an independent variable rather than plasma temperature. Based strictly on empirical correlations, Goldston and Kaye[15] found an average for the six tokamaks:

$$\tau_E \quad P_{HEAT}^{-0.58}$$

but the exponent value rang s on each of the tokamak machines examined from less than -0.3 to about -0.7, and it is this range which is quoted in recent INTOR workshop contributions on the likely range for the exponential contribution to confinement degradation.[11] The P_{HEAT} in existing experiments is supplied by NBI primarily, with some RF heating data. This data fit is valid in a regime where auxiliary heating was at least twice ohmic heating and so it may be considered as a single confinement time, τ_{aux}, and could be used in the appropriate regime or more generally applied within the Goldston scaling, $\tau = (1./\tau_{aux}^2 + 1./\tau_{ohm}^2)^{-0.5}$.

The Doublet III empirical results[21] are normalized to total plasma current, I_p and elongation, $K^{0.5}$. Their regression data fit appropriately to either of two forms: 1) $a+b/P_{IN}$ or 2) $a\ P_{IN}^{-b}$. Each form was used to fit limiter and then divertor runs separately. We assumed an alcater-like scaling proportional to minor radius squared in order to normalize the Doublet results to the INTOR-size device. This gave optimistic results, but results would have been even more optimistic if we had chosen the neo-alcator scaling (a R^2) to normalize.

The question of including alpha heating is not resolved. From theoretical grounds, confinement degradation is predicted due to the anisotropic deposition of energy in the plasma, leading to microinstabilities, turbulence, and thus to confinement degradation.[19] One might argue that alpha energy deposition is expected to be more nearly isotropic so that it would not contribute to anisotropically induced turbulence and thus not significantly decrease the confinement time. A separate theoretical speculation[22] suggests anomalous energy loss due to a temperature gradient driven mode. Then,

pessimistically, alpha heating may be included in P_{HEAT} and may, in fact, contribute to the steepest temperature gradients and thus the greatest energy losses.

The most important determining factors regarding the application of a scaling law are: (i) the value of the constant coefficient, (ii) the device size parameter dependence, and (iii) confinement degradation with input power P_{in} or with power density (T) or with both (as Ohkawa suggests). Another critical issue which will be discussed extensively is whether to include the alpha heating power in the auxiliary heating term that results in confinement degradation.

3. DISCUSSION OF RESULTS

3.a. Confinement Uncertainties

The eventual utilization of a tokamak reactor as a commercial power source necessitates an understanding of operational requirements during full and fractional power operations. The analysis of the time dependent fractional power operation of a tokamak relies upon the ignition characteristics of the device. These in turn vary with the form assumed for the energy confinement scaling law.

There are four major areas of uncertainty regarding confinement time:

1) What is the appropriate constant coefficient and size dependence to be used? τ_E, when extrapolated to reactor regime, is very sensitive to this coefficient, ranging from less than 0.5 to greater than 3 seconds which shifts the minimum ignition density from well above 10^{20} m^{-3} down to values only a few times 10^{19} m^{-3}.

2) Does τ_E degrade with alpha heating power? If yes, then an INTOR-size device will not ignite, and even in the more favorably scaled high density

compact tokamak ignition experiment designs, ignition may be marginal. Theoretical arguments have been made on both sides, that alpha power does (anomalous transport is due to temperature gradient driven MHD instability) or does not (anomalous transport is driven by microinstabilities and turbulence due to anisotropic heating) degrade confinement.

3) Should the experimentally observed degradation of τ_E during auxiliary heating scale with the auxiliary power level itself or with the increasing temperature of the plasma? While these are, of course, intimately related, the ignition contours, power output, and thermal stability regions differ significantly between the two assumptions. The current convention, to scale τ_E inversely with auxiliary power, is pessimistic when extrapolated to reactor regimes. If one scales τ_E inversely with plasma temperature, then ignition requirements may be less severe, and an ignited region of thermal stability is simultaneously provided.

4) What is the partitionin of energy transport between electrons and ions? Neoclassical ion confinement gives the most optimistic ignition results since the long time residence of the ions allows for a hotter ion species. Recent results indicate that ion energy confinement may in fact be anomalous and comparable to that of the electrons.[6] We found for this case of anomalous ion transport and when τ_E is degraded by auxiliary heating, that the INTOR plasma does not ignite unless the auxiliary heating is turned off in the ignition region. As ion confinement time is assumed to increase relative to that of the electrons, then ignition is achieved at decreasing densities and for decreasing amounts of required auxiliary power. At $\tau_{Ei} \sim 3 \times \tau_{Ee}$, ignition is found to be possible at $\bar{n} \sim 4 \times 10^{19}$ m^{-3} and requires ~15 MW auxiliary drive power, if auxiliary power degrades confinement.

3.b. STEADY STATE ANALYSIS

3.b.1. Ignition Contours

Contours of fusion reactor operating parameters are generated in the (n-T) space at thermal equilibrium for a wide range of confinement scaling laws including Alcator/INTOR, Goldston, Ohkawa, neo-Alcator, and Doublet-III scalings.

The ignition contours are the loci of equilibrium points in the density-temperature space where the driving auxiliary power is zero. The ignition contours for the several scaling laws are compared in Fig. 1 and for the Doublet scaling laws in Fig. 2. Scaling laws which degrade confinement with auxiliary power include only ohmic power at these ignition curves. Alpha power is excluded in these initial considerations except as noted on two of the Doublet scaling laws.

Scaling laws in which alpha heating does not disturb confinement allow ignition in either INTOR-sized or compact-tokamak devices. If auxiliary power degrades energy confinement time, then large auxiliary power sources (greater than 50 MW), will be required to achieve ignition. In this case, a unique ignited operation results in that adding auxiliary power causes a large increase in transport losses and thus a net loss of the plasma pressure, while decreasing auxiliary power improves confinement and thus leads to a net gain in plasma energy. This will be discussed in detail in Sec. 4.

There is a very wide range in the ignited operating point depending on the particular scaling law. The Mereshkin law is very optimistic, probably due to the major radius cubed scaling and shows ignition at densities as low as 0.2×10^{20} m^{-3}. The Ohkawa scaling is most pessimistic in terms of density-temperature ignition requirements but still allows ignition at a density of about 1.2×10^{20} m^{-3}. This scaling and that of INTOR/Alcator are

similar and both ignition curves coincide in a region where net reactor power is greater than zero. This will be discussed further in a following section. The Ohkawa and Mereshkin laws, with their $T^{-0.5}$ dependence, show a slightly positive slope of the ignition curve with temperature. This is an important feature for thermal stability and will be discussed further in a later section.

The Doublet scalings in Fig. 2 tend to be more optimistic overall. The worst case shows a limiter data fit to ($a\ P_{IN}^{-b}$), and ignition at densities of about 0.75×10^{20} m^{-3}. The Doublet scaling in the form, $a+b/P_{IN}$, is the only scaling which allowed ignition to be achieved when the alpha power is included in P_{IN}. These curves are also included in Fig. 2. In these cases, the alpha power degradation of confinement time adds a small positive slope in the ignition curve with temperature which allows for thermal stability at an ignited operating point.

3.b.1.i. Confinement Degradation with Alpha Power. We investigated the ignition condition for the most conservative case in which confinement time is degraded by alpha power, because of recent interest in an ignition device, particularly a compact tokamak. For this analysis, we considered a simple, single plasma species, zero-dimensional model examining both the Goldston scaling and the Kaye-Goldston scaling for confinement. It was assumed that at ignition, plasma heating comes entirely from the fusion alpha power P_α. Results are compared for the INTOR-sized tokamak and two design variations of the compact tokamak, the IGNITOR and the Brand-K compact tokamak. Characteristics of these devices[23] are listed in Table I. The simple model is appropriate to pick out the most salient features of the ignition comparison. More detailed analyses have been completed at ORNL.[24]

Goldston Scaling

With reference to Table II, according to Goldston scaling, at ignition $\tau_{ohm} > \tau_{aux}$, and

$$\tau \sim \tau_{aux} = bP^{-0.5} \tag{30}$$

The ignition condition equates fusion alpha power with total plasma loss which is to a good approximation just the transport loss; so ignition implies the zero dimensional power balance, which can be written as, assuming $T_i \sim T_e$ and $n_i \sim n_e$

$$K_\alpha n^2 \sigma v(T) = \frac{3nT}{\tau} \tag{31}$$

Substituting for τ

$$K_\alpha n^2 \sigma v(T) = \frac{3nT}{bP_\alpha^{-0.5}} = \frac{3nT}{b} P_\alpha^{0.5} \tag{32}$$

From this equation:

$$K_\alpha n^2 \sigma v(T) = \frac{3nT}{b} (K_\alpha n^2 \sigma v(T)\ V_p)^{0.5} \tag{33}$$

The ignition condition can be written as:

$$K_\alpha \left(\frac{\sigma v(T)}{T^2}\right) > \frac{V_p}{b^2} \tag{34}$$

The LHS of Eq. (34) includes the temperature dependence while the RHS includes the characteristics of a specific tokamak device and the transport scaling law. The LHS and RHS for each of the three tokamaks described are

plotted together in Fig. 3a.

Clearly, for the simple global comparison none of the devices achieve ignition. Their losses exceed the available fusion power by factors, respectively for INTOR, IGNITOR, and Brand-X, of about 3,2, and 1.4. An obvious improvement that can be made is to include the profile effect. By centrally peaking the density and/or temperature profile, we can increase fusion power while retaining the same plasma average temperature. Note that the plasma gain increases linearly with fusion power, and the plasma transport loss increases as the square root of fusion power. Thus, at constant average temperature the gain to loss ratio increases by the square root of fusion power gained by centrally peaking the profiles.

The device, Brand-X, is the closest to ignition, and from Fig. 3a, its closest approach to ignition is at $T \sim 13$ keV, where its loss is almost 40% greater than its gain. At this point, Brand-X is marginally ignited if its fusion power doubles (gain/loss = $2/\sqrt{2} = \sqrt{2} = 1.4$ giving the required 40% increase) due to the profile effects. Likewise, Ignitor would require a profile dependent fusion power three times more than the average plasma fusion power and INTOR six times more than to reach ignition.

Fusion power increase with centrally peaked profile shaping of density and/or temperature could be fairly large. The factor of two required for the Brand-X to reach ignition could be achieved, for instance, with profile factor exponents [see Eq. (11)], $pf_n = 0.25$ and $pf_t = 0.7$, which appears feasible. If both profile factors are equal to one, the fusion power increase with profile modification is about 3.6 but these profile factors may be unrealistically large.

Thus, considering the improvement in fusion gain with profile dependence, ignition is likely (but only marginally) in the Brand-X, ignition is not

likely but possible for strongly centrally peaked profiles in the IGNITOR, and extremely improbable in the INTOR-sized tokamak, given the Goldston confinement scaling law and that fusion alpha power is included in the heating power term.

Kaye-Goldston Scaling

For Kaye-Goldston scaling (see Table II), the density dependence of τ is weak ($\tau \sim \bar{n}^{0.26}$). Following an analysis similar to that given for the Goldston case results in an *ignition* condition given by:

$$k \frac{ov^{0.42}}{T} \geq \frac{vol^{0.58}}{K_{KG} n^{0.1}} \tag{35}$$

where k is just a unit conversion factor and K_{KG} is from the device dependent parameters found by writing τ as:

$$\tau = K_{KG}(n_e/10^{19})^{0.26} P_{TOT}^{-0.58} \tag{36}$$

For the three tokamaks of concern, K_{KG} is given by 4.23, 1.4, and 0.78, respectively, for INTOR, IGNITOR and BRAND-X. Using these values of K_{KG}, the plots of the LHS and RHS of Eq. (35) (for each device) are shown in Fig. 3b evaluating the RHS at $n = 10^{20}$ m^{-3} for INTOR, and at $n = 5 \times 10^{20}$ m^{-3} for the two compact tokamaks.

The fusion power is less than the transport losses by almost a factor of two for the INTOR device. This might ignite given realistic profile dependence of the alpha fusion power. The plasma power losses are less than the gains for the compact devices, so they achieve ignition under this scaling law. The INTOR ignition margin [defined here as the ratio of fusion power to plasma transport power, i.e., the LHS/RHS for Eqs. (34) and (35)] increases by

50% in going from the Goldston to the Kaye-Goldston scaling. For Brand-X and IGNITOR the improvement in that margin going from Goldston to Kaye-Goldston scaling is respectively, 250% and 280%. Improvements in compact tokamak performance suggest that the density and the plasma current dependences are the key factors. It is important to note again this apparent improvement relies upon extrapolation to a regime well beyond that of the data base. Extrapolation of regression results this far from the data can be misleading.

The brief analysis above comparing INTOR-size tokamaks and two recent designs for a compact tokamak ignition experiment suggests that ignition, even when it is possible in the compact tokamaks, is marginal if alpha power degrades confinement.

Since this class of confinement generally results in unignited plasmas, a reactor would operate as a driven machine. Thermal stability exists at all n-T points, but the device Q (= P_{fus}/P_{aux}) is low (<10). As a result, fractional power operation is controlled by the ion fueling rate, and the net power is limited by the available auxiliary power.

3.b.1.ii. Weak Confinement Degradation with Alpha Power. An interesting question is what effect partial alpha degradation of confinement has on ignition. A related question is: what is the maximum fraction of alpha power that can degrade confinement and still achieve ignition in an INTOR-sized tokamak. These questions are answered in a series of time dependent runs, with the average plasma temperature shown versus time in Fig. 4.

These runs employ Goldston scaling where: $P_{HEAT} = f_\alpha P_\alpha + P_{aux}$. Auxiliary power is used to linearly ramp the plasma temperature into the 'ohmically-heated ignition region' (about 6 keV at time = 4 sec.) at a constant density of 1.5×10^{20} m^{-3}. At that point auxiliary power is shut-off, $P_{aux} \rightarrow 0$, so $P_{HEAT} \rightarrow f_\alpha P_\alpha$ and the effect of varying f_α is determined.

The results in the figure indicate for $\bar{n} = 1.5 \times 10^{20}\ m^{-3}$, that if f_α is greater than some critical fraction, f_c, shown here to be $\lesssim 0.2$, then ignition will not occur, and the temperature relaxes to the ohmic-heating equilibrium of about 2.5 keV. The $f_\alpha = 0$ curve confirms that a very rapid thermal runaway occurs if no alpha power degrades confinement and if P_{aux} goes to zero while operating in the "ohmically ignited" region of n-T space.

The curves for $f_\alpha = 0.05$ and $f_\alpha = 0.15$ indicate that for $(0 < f < f_c)$ then alpha power degradation of confinement acts to establish an equilibrium temperature of the plasma which can be in the desirable operating range. In this example, for $f_\alpha = 0.15$ the temperature approaches a thermal equilibrium at ~ 12-13 keV. This suggests that a nominally optimum operation at ~ 10 keV might be achieved for $f_\alpha \sim 0.16$.

Of course, at this time, little is understood about the mechanisms for alpha power-degraded confinement. The above simple example suggests, however, that if the fraction, f_α, can be controlled in some manner by manipulating other plasma parameters, then the benefit is immense. Maintaining f_α less than a critical value, f_c, we assume that ignition can be achieved, and if f_α can further be controlled to take on an optimum value (about 0.16 in this example), then thermal stability in the ignited region is assured. These goals should be kept in mind in guiding future experimental and theoretical work on ignition devices.

In summary, if the total alpha power is responsible for confinement time degradation in a form such as $\tau \sim kP_\alpha^{-x}$ for $x \sim 0.5$, then ignition will not be achieved in an INTOR-scale tokamak. However, there are the two exceptions: first, if τ scales as the most optimistic Doublet-III law ($\tau \sim a + b/P_{HEAT}$), and second, if only a small fraction, found to be about 15-20%, of the alpha power is assumed to degrade τ. The latter argument may indeed be realistic,

given that the alpha power produces isotropic heating in velocity space and that only anisotropic heating contributes to τ degradation.

A net electric power output from the reactor is possible at low plasma gain factor, Q, for the case with $f_\alpha > f_c$, where the reactor is subignited. Fractional power operation is attained simply by controlling the density via the ion source and the temperature via auxiliary power in an n-T regime which is everywhere thermally stable. If $f_\alpha < 20\%$, ignition is possible in an INTOR-size device, while thermally stable ignited operation is found only for an optimum $f_\alpha \approx 15\%$.

3.b.1.iii. Ignition Sensitivity to Ratio of Ion to Electron Confinement Times. As indicated in Sec. 2.c., we have used semi-empirical scaling laws to model the global energy confinement time. The appropriate partitioning of transport losses between conduction (τ_E) and convection (τ_p) or between electrons (τ_e) and ions (τ_i) is not well known. Therefore, these partitions can be varied within a range consistent with experimental uncertainties, so long as the total net transport loss agrees with the specified global scaling law.

Varying the ratio of τ_i/τ_e is expected to have a substantial impact on the ignition condition, since a longer τ_i implies a greater ion to electron temperature ratio. This implies greater fusion power for a fixed total transport loss dominated by losses through the electron energy channel. Thus, ignition can be achieved in a region with lower average density and temperature.

This phenomenon is examined for the Goldston scaling law with confinement time degraded by auxiliary power only. The results are shown in Fig. 5, which includes, as a base case, the ignition curve for $\tau = \tau_{ohm}$ with Goldston scaling and $\tau_i/\tau_e = 1.5$. With $\tau = \tau_{aux}$, the ignition condition is much more

severe than for the base case, for the same τ_i/τ_e. As τ_i/τ_e increases, ignition condition improves such that at $\tau_i/\tau_e \sim 5$, ignition condition for $\tau = \tau_{aux}$ is comparable to that of the base case at low densities, and nearly comparable at higher densities and lower temperatures. Likewise, when τ_i/τ_e decreases towards unity, ignition degrades rapidly. In particular, for $\tau_i/\tau_e \sim 1 - 1.1$ ignition does not occur for the case $\tau = \tau_{aux}$.

Figure 5 also indicates the approximate level of auxiliary power required to reach ignition, assuming that auxiliary power is applied throughout. While this required power is prohibitively large as τ_i/τ_e approaches unity, it can be reduced to an acceptable level by turning off the auxiliary power once it reaches the ohmic ignited region (above the $P_{aux} = 0$ curve in Fig. 5).

Models of plasma power balance often assume nearly neoclassical energy loss for the ions which would give a large τ_i/τ_e and thus very optimistic ignition results. Recent experimental results[6] indicate ion loss may also be anomalous implying $(\tau_i/\tau_e) \sim 1$. One can conclude that definitive understanding of ion transport is still absent at present, and future experiments to investigate the underlying physics are needed. It should be borne in mind that operating in the hot ion mode ($T_i > T_e$) results in better utilization of plasma β.

3.b.1.iv. Ignition and Auxiliary Power. The scaling laws lead to a wide range of methods for fractional power operation and the laws are conveniently grouped for analysis into three classes:

1) Confinement time is independent of any heating power.

2) Confinement time degrades with increasing auxiliary heating power.

3) Confinement time degrades with total heating including auxiliary and the fusion alpha power heating.

Confinement in class 1 (tau independent of heating) or class 2 (tau

dependent upon auxiliary heating) will have the same ignition curve in n-T space because at ignition, auxiliary power is set equal to zero. Class 2, however, has two greatly different solutions for equilibrium power as a function of density and temperature. One solution is valid when auxiliary power is off (then this class is the same as class 1) and another when auxiliary power is on. As long as auxiliary power remains on, and within realistic maximum power limits of the auxiliary drive, then class 2 confinement remains unignited for Goldston and similar scaling laws. This leads to a strategy for class 2 ignition, first, the plasma is heated to a region in n-T space that would be ignited if there were no auxiliary power on. Then the auxiliary power is shut off which greatly increases tau, decreasing power transport losses, and thus the plasma becomes ignited.

Within these classes of confinement, the ignition curves cover a wide range of n-T space, and are similar to those that would be generated assuming that $0.5\ s < \tau < 4\ s$, as shown in Fig. 6. The areas above each ignition curve are shown in the figure, where thermal equilibrium can be achieved by increasing transport losses by 10%. This area is evaluated by comparing the equilibrium power contours (Fig. 7) and the transport power contours (not shown).

Equilibrium power contours are given in Fig. 7, and they show that it is generally not possible to operate, due to thermal instability, at locations of n-T points which are significantly above the ignition curve. These points have negative values of equilibrium power and are therefore accessible only if large amounts of power are removed from the plasma. Additionally, their points are thermally stable only if the net power balance has a positive temperature coefficient, that is, $dP_{net}/dT > 0$ for stability. Since P_α increases with T, then P_{LOSS} must increase with T faster

than P_α increases for thermal stability. The operating points marginally above the ignition curve are accessible by either decreasing the fusion power (obviously not desirable from output considerations) or by increasing the transport losses in order to avoid thermal runaway.

Thus, the operating region defined in a density-temperature space is generally limited to a small margin near the ignition curve. The ignition curve may be varied by changing transport or radition power losses. Severe thermal instability problems are expected in the low temperature, high density region near ignition. This leaves only the option of increasing reactor power levels by increasing temperature so that the operating point stays near the ignition curve in the lower density region. The time dependent studies which will be described indicated that control of the operating point in this region can be achieved by an active feedback control synchonizing the ion fuel source injection with the auxiliary power source. Each system must be controlled in such a way as to keep the reactor marginally ignited.

There is a penalty in increased auxiliary power requirements for shorter confinement times. A short confinement time, which is just long enough to achieve ignition, may be desirable to increase transport losses so that larger values of n-T space can be made thermally stable. The auxiliary power increase with decreasing constant values of confinement time is shown in Fig. 8. These values of maximum power correspond to the values at the "saddle point" of auxiliary power as seen clearly in the plot of Fig. 7.

3.b.2. Reactor Parameters in (n-T) Space

It is helpful to consider contours of several reactor parameters in (n-T) space when designing a reactor and evaluating its thermally stable mode of operation. Such parameters include auxiliary power, net equilibrium power, net electric power, fusion neutron wall loading, confinement time, and so

on. A complete set of these contours is generated for each scaling law case; for example: 1) Goldston scaling, ohmic-only, which is a simple and optimistic case, 2) the complete Goldston scaling with auxiliary power degrading confinement time, and with $\tau_i/\tau_e \sim 1.5$, and 3) the complete Goldston scaling with auxiliary power degrading confinement and $\tau_i \sim 1.1 \times \tau_e$. From these parametric figures all relevant operating values can be determined for reactor design.

Figure 9 compares the auxiliary power surface contours for these three cases and also for Kaye-Goldston scaling (at $\tau_i\ \tau_e = 1.1$). Case 1 achieves ignition easily, case 2 achieves ignition but requires considerable auxiliary power, and case 3 does not achieve ignition. The Kaye-Goldston scaling produces results similar to the Goldston at $\tau_i/\tau_e \sim 1.5$. Of course, the cases 2 and 3 can reach ignition by simply shutting off the auxiliary power once they are in the (n-T) region ignited for case 1, since with $P_{aux} = 0$, these cases 2 and 3 are equivalent and revert to case 1. For comparison the surfaces of reactor net electric power for each case are included in the figure.

The key design parameters are taken from the Goldston contours and shown in Fig. 10. The beta limit of 3.5% sets the operating limit on our (n-T) point. In this region, the net electric power curves of $P_{net} = 0$, and $P_{net} = 250$ MW are shown. Several possible ignition curves are overlaid as well to show the differences in power levels accessible at ignition for different confinement scaling law assumptions.

3.b.2.i. Ignited Operating Restrictions. The operating restriction to n-T points near the ignition curve has a most significant effect in relation to the contour plots of constant fusion (or net electric) power. The device must be engineered in such a way that the resulting ignition curve coincides

in the n-T space as closely as possible to the range of output power curves desired from the device. The design trade-off is that as one improves confinement, then less auxiliary power will be required to reach ignition, but then also the ignition curve will decrease in n-T space leaving the regions of greater output power farther into the more thermally unstable and thus inaccessible region of n-T space. Thus, with the correct scaling law known for a particular device and the auxiliary power limits given, then the device output power can be optimized, subject to the thermal stability constraint of operation near the ignition curve.

3.b.3. Thermal Control by Impurity Radiation

In the event a reactor is overdesigned it may reach ignition at n-T points well below regions where net electric power output is possible. Those desirable (n-T) regions could be reached by spoiling confinement as we have discussed by increasing transport losses by a number of mechanisms. Another possibility is spoiling ignition by increasing radiation losses through intentional high-Z impurity injection. This was considered in the STARFIRE tokamak study.[25] An allowable impurity concentration can be determined as a small fraction of total plasma beta, say 10% which will be tolerated for the impurity. This will result in an acceptably small reduction to net reactor power (assumed for our simple analysis only, 10% beta means about 20% cut in power which is probably not economically acceptable).

Using a guideline of <10% of total beta, it is easy to determine that bremstrahlung radiation will not produce enough power loss to ignificantly change the (n-T) operating point. Sufficient radiation could only be lost through line and recombination radiation from a very high-Z impurity which is incompletely ionized even at 10 keV. In STARFIRE, iodine was proposed to be injected. It is difficult to predict accurately the degree of ionization, but

the radiation power parameter for this material can be estimated from data in the literature.[26] Our rough estimates assume an average of 30 electrons stripped from the iodine atoms, and a radiation power parameter, $Q_I(T=10keV) \sim 4 \times 10^{-32} W \ m^3$. These values indicate that iodine should easily provide radiation losses sufficient to spoil confinement as needed, without serious depletion of the plasma beta required for the ion fuel. The iodine concentrations are low so for confinement time comparable to fuel ions the required injection rate will be relatively small, and burn control by impurity injection appears reasonable.

The INTOR group examined this issue[8] and found it impractical because of short impurity confinement times (comparable to the fuel ions) required and excessive demands on the impurity injection systems for diagnostics and feedback control. They considered iron atoms as the impurity, but the much higher Z impurity, iodine, gives significantly more radiative loss and might relax the injection system demands to tolerable levels. In the more recent summary of the American contribution to INTOR[11] this issue was not addressed.

It is important to note that the line and recombination radiation, P_{LR}, have negative temperature coefficients, that is $dP_{LR}/dT < 0$. This means that even if impurities were added to achieve a net power balance at the desired (n-T) operating point, that operating point would not be thermally stabilized by the radiation losses. A slight increase in temperature would cause less radiative loss and thus further temperature increase until either the beta limit was reached or until bremstrahlung radiation increased with temperature to arrest thermal runaway at a significantly higher temperature (>20 keV).

3.b.4. Thermal Control by Divertor Mode Operation

We now briefly discuss the possibility of maintaining plasma thermal control by varying the mode of divertor operation. Good energy confinement,

termed the H-mode, has been observed on several tokamaks running with a divertor, including ASDEX,[27] D-III[28] and PDX.[29] It is characterized by low neutral recycling at the edge, which allows for low impurity, low scrape-off temperature and high density at the divertor plate. A divertor plasma may operate in the H-mode or have low confinement (L-mode), while limiter operations have only achieved L-mode confinement. The transition between L- and H-mode is not completely understood but is a complex problem relating the plasma edge physics as a boundary condition to the core plasma transport.

A reactor operating in L-mode or H-mode will have a distinct ignition curve in each mode, as was seen in Fig. 2, showing similar scalings for D-III.

Provided that the divertor can be controlled by external means, it might be possible to obtain a time-averaged ignition curve anywhere between the two ignition curves for L and H mode. The time-averaged ignition curve is considered because it may only be possible to alternate between a full H or full L mode operation but with a controlled duty cycle, effecting a time-averaged intermediate mode operation.

Since H-mode is more favorable for ignition, a reactor can be ramped up to ignition in the H-mode. If the ignition point is below (in n-T space) the points of desired net power output, the ignition curve and operating point could possibly be raised by shifting to L-mode operation. This might, for example, be effected by varying the spatial orientation of fuel injection by gas puffing or pellet injection variations. Thus, L-mode operation might allow thermal stability in regions of n-T space that would otherwise be inaccessible due to thermal instability.

4. TIME DEPENDENT ANALYSIS

We now consider the dynamics of moving a reactor plasma through a

trajectory of n-T points to reach the point of desired output power. Since power operation is limited to a region near the ignition curve there are two distinct ways to approach the fuel power: 1) at lower density with increasing temperature, or 2) at lower temperature with increasing density. The first approach is in a more thermally stable regime and thus favorable from a reactor control viewpoint, but the second approach permits greater net power for a given beta value (i.e., greater maximum power at the beta limit). This is more favorable economically. Time evolutions of plasma parameters along these optional paths were studied with the time dependent code. The results are summarized in the following sub-sections, starting with the simple case in which we assume a 'soft' beta limit.

4.a. Soft Beta Limit

This case was analyzed assuming Goldston scaling with auxiliary power degradation. A 'soft' beta or non-disruptive beta limit was modeled by making τ dependent upon β so that it degrades rapidly as the β approaches the critical beta limit β_c, $[\tau(\beta,n,T) = \tau(n,T)\ \exp(-1\ (\beta/\beta_{crit})^{**}10)]$. Near the beta limit, transport losses increase until thermal equilibrium is achieved with saturation in beta, and thus restricts further increase in temperature. The time dependent analysis confirmed that this case is thermally stable at the beta limit even at points well above ignition. The n-T trajectory for such a case is shown in Fig. 11 followed by the time variations of the major operating parameters, shown in Figs. 12 a-f.

At times, t = 0.-11.5 s, the ion source and auxiliary power are varied to achieve linear density and temperature ramps in time until ignition is reached. (Note that this scenario is not optimized, and that a slower ramp rate to ignition would greatly reduce that peak auxiliary power from the level shown in Fig. 12b.) At t = 11.5 s, the auxiliary power is turned off,

transport losses decay rapidly with half-life of the energy confinement time. At t = 12.5 s, the temperature falls briefly until the alphas thermalize sufficiently to restore ignition. At 13.5 s, the temperature increases rapidly through the ignited n-T space until the beta limit of 3.5% is reached.

In the interval, t = 13.5 - 18. s, the density continues to increase at a constant rate, and the operating point moves up in density along the isobaric contour at the beta limit. This isobaric movement is stable, and thermal equilibrium exists at all points. At t = 18.0 s, a preprogrammed control sequence causes the steady-state plasma current to drop by 10%, which forces the beta limit and thus the temperature to decrease at constant density accordingly to the new lower Troyon beta limit. In the last interval, t = 18.2 - 20. s, the density continues to increase isobarically along the contour at the new beta limit of about 3.2%.

This operating point remains thermally stable at all times for any specified density up to the Murakami density limit. It is important to recall, with reference to Fig. 10, that as we increase the n-T point isobarically in density we are also increasing the net reactor electric power output.

Trajectories in n-T space for this case can be controlled by varying the ion fuel source, and thus moving up or down in density along the isobaric contours. The contour for the desired trajectory can be varied by changing the beta limit. Assuming a Troyon beta limit, a lower value can be achieved by lowering the steady state plasma toroidal current, which will then in turn shift the beta-limited operating point to a lower temperature at constant density. It is, therefore, clear that a 'soft' beta limit, if it exists, can provide an excellent scheme for passive feedback burn control.

4.b. Active Feedback Control for Thermal Stability (in low density high temperature region)

Two trajectories are shown for Goldston scaling: the first, in which thermal equilibrium is not achieved, is shown in Fig. 13, and the second, in which equilibrium is achieved, is shown in Fig. 14. The time evolutions of the key parameters for the second case are then shown in Figs. 15 a-g.

In both cases, once ignition is reached, density is controlled so the operating point remains on the ignition curve. This point is thermally unstable and so the temperature drifts, slowly increasing. When 10 keV is exceeded, the feedback system is programmed to decrease density further by simply cutting off the ion fuel source until the operating point falls out of ignition and the temperature is allowed to swing back down below the 10 keV point. Once below 10 keV, the ion fuel source is turned on again so that the density is increased, and auxiliary power is added to return to the ignition curve. This is apparent in the first trajectory, shown in Fig. 13. Using this simple feedback scheme, and owing to the slow thermal response time of the plasma in this regime, the n-T trajectory does not equilibriate quickly. The first trajectory returns to the ignition curve at a higher density value and well below the 10 keV trigger point (indicated as point A in the figure). From here, ignition leads to thermal runaway. Even with no ion fuel source, the density does not drop fast enough during the temperature excursion to bring the operating point back out of ignition again, before the plasma beta limit is exceeded. This example illustrates the extreme thermal instability of the ignited region at low temperatures and high density.

In the second trajectory (Fig. 14), the density is dropped only slightly below the ignition contour at the 10 keV trigger point. The slow temperature excursion falls below 10 keV while a constant density is maintained in the

marginally subignited region. Then, when the density and auxiliary power are increased again, the trajectory returns to the ignition curve at an adjacent n-T value. Repeating this cycle, the operating point oscillates about T = 10 keV in an actively controlled thermal equilibrium, as seen clearly in the temperature verses time plot in Fig. 15a. If the plasma temperature ramp rate was maintained well below this thermal response time, the oscillations about the n-T equilibrium point could be entirely avoided.

The analysis confirmed that active feedback can be used to maintain a thermal equilibrium point just below the ignition curve. Modulating the ion fuel source in order to maintain the density at a point exactly on the ignition curve is insufficient to fix the operating point because equilibrium points on the ignition curve in this case are thermally unstable, and the temperature will slowly increase while the operating point remains on the ignition curve. Thus, thermal equilibrium requires an operating point just below the ignition curve which must be maintained by a synchronized feedback of both the ion source and the auxiliary power.

The thermal response time of the plasma near ignition is slow (several seconds) owing to the small net power. The simple feedback scheme used here resulted in large fluctuations in the net power output due to the pulsed auxiliary power. It is believed that a more sophisticated feedback scheme with proportional control could be used to reduce the output power fluctuations to acceptible levels (and this should be investigated in future work).

If we had assumed that confinement time degrades with auxiliary power the feedback scheme is expected to be similar but with larger amounts of auxiliary power required as the plasma drops marginally out of the ignited mode. In that case, a good feedback scheme would be even more essential in reducing

output power fluctuations, and it may be difficult to reduce the power fluctuations in that case to acceptable levels.

In these cases, thermal equilibrium can be maintained at any poi t near ignition up to the beta limit which determines the maximum power output value. Transition between fractional power levels is relatively simple. By shutting off the feedback scheme when marginally subignited, the temperature and the net output power level will drop. By shutting off the feedback when marginally ignited, or by maintaining the density exactly at ignition, then the temperature will rise and with it the reactor power will increase in a controlled manner.

4.c. Active Feedback Control for Thermal Stability (in the high density, low temperature region)

For the case where confinement is independent of heating power, we were unable to maintain thermal equilibrium in this n-T region even with active feedback control working to keep the operating point marginally sub-ignited. This confirms expectations that the region is unconditionally thermally unstable. For thermal stability one would have to move to a point on the low power side of the hump in the sub-ignited auxiliary power contours, and would thus end up with a driven device operating in a region far from the desired net power output contours.

One may operate in this ignited region, however, if confinement time degrades with increasing auxiliary power. Time dependent studies confirm that thermal equilibrium can then be maintained by supplying the appropriate amount of auxiliary power. Adding auxiliary power can increase the transport losses so dramatically that the temperature of the plasma decreases, while cutting back on the auxiliary power will improve transport losses so that an ignited regime is again reached and the plasma temperature increases. Large

fluctuations in output power again result from the simple active feedback scheme, but a more sophisticated scheme should alleviate this problem. The operating point will be bounded by the Murakami density and by the Troyon beta limit.

The n-T trajectory is shown for such a case in Fig. 16, followed by the time dependent variations of operating parameters in Figs. 17 a-g. The density and temperature are ramped linearly as in the previous case, but much larger values of auxiliary power are now required. These values could be reduced significantly if allowing for smaller temperature and density ramp rates in time. Once the operating point is above the ohmic ignition curve (at about t = 5 s), the auxiliary power is modulated to maintain thermal equilibrium. Density increases until t = 10 seconds, then the source is adjusted to maintain a constant density at $\bar{n}$ = 1.5 x 10^{20} m^{-3}.

Reactor power output fluctuations, in Fig. 17g, would be large in this simple scheme, because of the large fluctuating power requirement on the auxiliary power feedback system. These power fluctuations cannot be reduced when operating at a point well above ignition to the extent shown in the previous case. Still, to some extent not yet determined, the observed power fluctuations can be reduced by refinement of the feedback scheme.

Fractional power operation in this mode is varied by changing density possibly along a contour of constant plasma equilibrium power. This mode requires additional work to clarify the conditions required to avoid thermal runaway. An important consideration for reactor operation in this mode is plasma control following a loss of auxiliary power. Such a loss would lead to an uncontrolled temperature excursion which might lead to a disruption as the plasma beta approaches the beta limit, unless a 'soft beta' limit prevailed. A counter argument might be that only about 20-30 MW of auxiliary power are

required to maintain thermal control, but much more power, (>100 MW) may be required to reach ignition. Thus, a "back-up" system of auxiliary power would be available to arrest a thermal runaway following the failure of the primary thermal control system. Thermal runaway times are on the order of seconds, so this back-up system could be implemented practically. Overall, however, the large magnitude of plasma power required to be removed for thermal equilibrium in this region makes it very thermally unstable, and thus undesirable as an operating region.

4.d. Confinement Degraded with Temperature

Confinement time may be scaled to degrade with increasing temperature or with increasing auxiliary power. Since these are intimately related, it is probably not appropriate to assume confinement time degradation with both simultaneously. The ohmic confinement time of Ohkawa (set $P_{IN} = 0$ in the evaluation of τ in Table II) shows a dependence of $T^{-0.5}$, which can be seen in Fig. 1 to provide an ignition curve with a slight positive slope with temperature above about 10 KeV. This assures passive thermal stability, provided that the density can be held constant in that narrow range (~1.1 -1.2 x 10^{20} m^{-3}) where the desired positive slope of the ignition curve exists.

This passively thermal stable region was examined in a series of time dependent runs at constant density. Temperature versus time results are shown in Figs. 18 and 19. Figure 18 shows T(t) for three sweeps, at different values of constant density. Figure 19 shows T(t) for $\langle n \rangle \approx 1.1 \times 10^{20} m^{-3}$, which was the minimum density required for ignition. The three runs here differ after t = 30 seconds, when the fueling ratio, deuterium atoms per tritium plus deuterium atoms, was reduced to decrease fusion power.

Examining first Fig. 18, runs at average density less than 1.1 x 10^{20} m^{-3} did not reach ignition. The constant temperature ramp at early time in each

case is the subignited region driven by feedback control to auxiliary power. The time dependence in this case of the ohmic and required auxiliary power are the same as that superimposed in Fig. 19, with $P_{OH}(t)$ and $P_{aux}(t)$ drawn qualitatively only. For higher density values in Fig. 18, ignition is achieved at lower temperatures. This ignition point is where the linear temperature ramp stops when auxiliary power is shut-off, and the plasma drifts to its own thermal equilibrium. As density increases from 1.1 to 1.2 x 10^{20} m^{-3}, the plasma equilibrium temperature increases from about 17 to 24 keV (assuming we are not restricted by plasma beta for this point). This seems to imply fairly accurate density control would be required to control plasma temperature relying on passive control in this regime. Also, the minimum stable ignited temperature possible in this manner is about 15 keV. Equilibrium points at lower temperatures are in a subignited and thermally unstable region.

Figure 19 shows that at the minimum ignition density of ~1.1 x 10^{20} m^{-3} we can reduce the equilibrium temperature to less than 15 keV, about 12-13 keV, by changing the fueling fraction from its value for optimal power density, 50%D/50%T, to about 40%D/60%T, reducing P_α by about 5%. Further reducing the fueling ratio, e.g., to 30%D/70%T causes the reactor plasma to fall out of ignition as shown.

The consequences of these findings to power operating scenario are discussed further in Sec. 5.

Without the non-disruptive beta limit, passively thermal stable operating regimes can be obtained by a driven sub-ignited reactor or by a temperature dependent confinement time (e.g., Ohkawa's scaling). Recent studies indicate that ripple-trapped particle banana modes do not offer the strong temperature dependence, as previously thought; thus, ripple losses do not guarantee a

passive thermal stability. The mechanisms which decrease confinement with increased temperature need additional study since they could be used to effect passive thermal stability control. Since temperature dependent confinement is not assured and the driven reactor may prove less economically attractive, we investigated active control points near the ignition curve in the representative confinement scaling given by Goldston.

Overall, the consequences of several possible confinement scaling laws on reactor operations at full and fractional power were investigated by examining relevant operating parameters in a steady-state region of density-temperature space and by following several time dependent analyses. The results suggest a range of methods for operating at different power levels and for transiting between adjacent power levels depending upon the confinement scaling in effect. Thermally stable operating points are limited to the sub-ignited regions and the marginally ignited regions along the low density side of the ignition contour. Unless a soft beta limit applies or confinement has a significant temperature dependence, a marginally ignited tokamak will need an active feedback control of auxiliary power and fuel ion injection in order to maintain thermal equilibrium at a point corresponding to the desired fractional power output of the tokamak reactor.

5. FRACTIONAL POWER OPERATION SCENARIOS

We choose to present possible operating scenarios as trajectories in (n-T) space superimposed upon contours of net electric power, P_{net}. The assumed values used to calculate P_{net} are listed in Table I, and P_{net} is defined as:

$$P_{net} = \eta_{th}(P_{\alpha} + 4 \cdot M \cdot P_{\alpha} + P_{aux} + P_{oh}) - P_{aux}/\eta_{aux} - P_{oh}/\eta_{oh} - P_{bas} \quad . \tag{41}$$

The value of P_{bas} = 150 MW is consistent with the INTOR (1982) value of 200 MW, which also includes P_{aux}/η_{aux} and P_{oh}/η_{oh}. The plasma heating power and the blanket multiplied neutron power, $4 \cdot M \cdot P_{\alpha}$, are recovered at a single thermal efficiency, η_{th}.

5.a. Confinement and Auxiliary Power

The trajectories for the two cases, namely confinement scalings independent of and dependent upon auxiliary power, are taken directly from the results in Sec. 4 and are shown together in Fig. 20. Net electric power (positive and negative value) contours are included as well as beta values of β = 3.5%, and β = 5% and the ignition curve, P_{aux} = 0, for Goldston scaling.

This illustrates the dilemma of an optimistic ignition curve. Ignition is achieved when the reactor has a net electric power output of about -100 MW, or 100 MW are needed to sustain operation. This is primarily due to the 150 MW assumed as a base-line or constant load requirement, thus the reactor is actually putting out about 50 MW of electric power near ignition.

For confinement time independent of auxiliary power (trajectory A), thermal stability restricts operation to points along the lower right side of the ignition curve. In this case, the full ignited reactor range of power is from about -100 MW to -60 MW. These points are stable only with active feedback of the ion fuel source and auxiliary power. Regions of greater power output are only accessible for stable operation if the ignition curve can be raised by increasing transport or radiation losses.

Trajectory B depicts the case for confinement time degrading with auxiliary power. In this case, feedback of the auxiliary power allows for active thermal control above the ignition curve. All (n-T) points can be made

stable with feedback up to the beta limit, thus all positive net power levels up to that limit are accessible. For the assumed $\beta_{max} \approx 3.5\%$ and $\langle n \rangle_{max} \sim 1.5 \times 10^{20}$ m^{-3} this reactor can operate along the 200 MW contour. However, this contour is for the ignited case and does not consider the auxiliary power needed to maintain the thermal equilibrium. It was found in the previous section that about 25 MW of auxiliary power was needed at the equilibrium position, $\langle T \rangle \sim 6$ keV, $\langle n \rangle \sim 1.5 \times 10^{20}$ m^{-3}. At this density and the temperature corresponding to the beta limit of 3.5% it is estimated about 50 MW are needed for thermal stability so the 200 MW contour there would be effectively reduced to about 150 MW. If the reactor were assumed to have larger stable beta, e.g., $\beta = 5\%$. then correspondingly larger net output power could be achieved but proportionately larger auxiliary power would also be required to maintain thermal stability.

5.b. Temperature Dependent Confinement

The time dependent studies described in Sec. 4.e can be summarized on a net electric power contour plot as shown in Fig. 21. Contours of beta, $\beta = 3.5\%$ and $\beta = 5\%$ are shown as well as the thermally stable operating points along the ignition curve, marked with the heavier line in the figure.

The time dependent study showed that the region labeled ($\Delta\langle n \rangle$) is thermally stable by varying the density against the effects of the temperature dependent confinement. The region labeled (Δfd) is thermally stable by varying the deuterium fuel fraction at constant total fuel ion density.

First, to operate a reactor for this scenario in an ignited, thermally stable region we must raise a beta limit to 5%, since at $\beta < 3.5\%$ there is no stable ignited region accessible. Then, we find there is a minimum power point for ignited thermally stable operation (at the left end of the heavier line, $\langle T \rangle \sim 14$ keV, $\langle n \rangle \sim 1.1 \times 10^{20}$ m^{-3}). Thus, in this scenario, (A, at

constant density equal to desired operating density) the reactor must power up rapidly to this point, with a net electric power output of about 300 MW. Alternatively, one could approach this stable operating point from lower densities at approximately constant temperature, in which case the reactor would be subignited and therefore thermally stable all the way to the ignited operating point (labeled B in the figure).

A middle road may be ideal (C), increasing density along the ohmic power equilibrium contour until the operating point reaches the minimum density at which $P_{net} = 0$ for some temperature. At this point, $\langle n \rangle \sim 0.85 \times 10^{20}$ m^{-3}, auxiliary power is added as needed to increase temperature at constant density until $\langle T \rangle \sim 14$-16 keV. At this point, operation is subignited, therefore stable, and net electric power output is zero, so there is no major penalty in staying at that point during start-up procedures or testing. Increasing the density now while proportionately cutting back on auxiliary power will bring the operating point up to ignition, while increasing net reactor power output.

5.c. Optimum Confinement Conditions

Three cases of "optimum" or desirable confinement conditions are shown together in Fig. 22, including: an ignition curve with a strong temperature dependence (A), an ignition curve which crosses the contours of desirable net electric power output (B), and the 'soft' beta case (C).

A temperature dependent ignition curve (like A in Fig. 22) is ideal in that net electric power levels from zero up to the maximum at the governing beta limit are thermally stable. This curve might be achieved with $\tau \propto aT^{-b}$, where comparison to the mild temperature dependence discussed for the Ohkawa scaling law indicates that $b > 0.5$ is needed. Ignition curves similar to this can also be generated by varying the coefficient and the exponent values (within reasonable experimental agreement) of a $\tau \sim aP_{IN}^{-b}$ type of scaling. As

discussed in an earlier section, if a small fraction of the alpha power degrades confinement time, then thermal stability is achieved, due to an ignition curve of this type. This underscores the need to understand the dependence of these values on controllable plasma parameters. The scaling dependence on temperature or auxiliary power, and the extent that alpha power degrades confinement can vary the ignition curve from the worst case of non-ignition to the optimal case with passive thermal stability at ignition and in regions of desirable net power output.

The best ignition curve (B in the figure) that may result if an inverse temperature dependence of confinement cannot be achieved, would be an ignition curve that coincides with (n-T) points of zero net power up to the maximum desired power output. Any point along this ignition curve could be maintained in equilibrium by active feedback as shown in the time dependent studies. Active feedback of the fuel source and auxiliary power would be required to achieve desirable power output levels.

The trajectory depicted in Fig. 11 for the case of a 'soft' beta limit is shown as curve C in the Fig. 22. That trajectory is extended here to points of greater net reactor power along the beta limit contour of 3.5%. Higher net reactor power would be achieved if a larger beta limit could be obtained.

The trajectory jogs slightly as it crosses the -100 MW contour, which is the transient effect of alpha thermalization at the point ignition is reached and auxiliary power is turned off. From there, the ignited plasma goes into a thermal runaway, but this is slow because the density is being continuously increased, and so too, the plasma heat capacity is increasing. The temperature increase continues until the beta limit is reached, where the increased transport losses result in thermal equilibrium, arresting the runaway at a temperature of $\langle T \rangle \sim 19$ keV in this case. The ion fuel source is

kept on and the operating point moves to higher density, being constrained to the beta limit contour. The plasma current was then arbitrarily decreased at $\langle T \rangle \sim 17.5$ keV. The Troyon beta limit decreases proportionately and the temperature drops rapidly to the temperature of the new beta limit. The density then continues to increase isobarically on this new beta limit until the assumed Murakami limit on density is reached.

The operating point can then be varied with temperature at constant density simply by changing the beta limit through increasing or decreasing the plasma current. It is important to note that all ignited points within the density and beta limits are inherently thermally stable, thus eliminating the need for burn control. Operating close to the beta limit will allow higher levels of net reactor power as we move isobarically to the low temperature, high density region: thus, the maximum power will generally be set by the density limit. In this case, at $\langle n \rangle_{max} \sim 1.5 \times 10^{20}$ m^{-3} the reactor could produce about 200 MW net electric power.

The problems of thermal stability in reactor power operation disappear if a soft beta limit is attainable. The plasma increases its transport losses as its beta value approaches a critical beta limit in such a way that thermal equilibrium is maintained. A passive mechanism for obtaining a 'soft' beta limit based on better understanding of plasma transport properties would be an ideal method for power control. On the other hand, an active feedback scheme; for instance, increasing ripple losses as the plasma beta approaches its critical value, may also be considered. Such a scheme has been examined previously[11] and was found to require large engineering modifications to the TF coil systems. However, both schemes involve large amounts of heat flux on the outer edge of the plasma that may impact the required heat removal capabilities of the divertor/limiter system. A detailed trade-off study

between the plasma and engineering constraints is needed to address this issue.

6. DISCUSSIONS AND CONCLUSIONS

The eventual utilization of a tokamak fusion reactor as a commercial power source necessitates a thorough understanding of the operational requirements at full and fractional power levels and during transitions from one operating level to another. In this study we examined the role of burn control in maintaining the reactor plasma at equilibrium to avoid thermal runaway during these power operations. Because these requirements rely so heavily upon the assumptions that govern plasma transport, this study focused on time dependent analyses and burn control using a range of energy confinement scaling laws. A comparison of ignition criteria for these scaling laws was also presented.

Steady-state analyses indicate that to achieve passive thermal stability in an ignited plasma the operating region is restricted to the low density, high-temperature portion of the ignition curve and thus severely limits the reactor net power output. Time dependent studies show that even in this region thermal stability requires active feedback of the ion fueling and auxiliary power. Increasing reactor power is achieved by increasing temperature at nearly constant density up to the beta limit. Burn control requirements are relaxed greatly if we allow for a 'soft' beta limit, wherein the transport losses increase without plasma disruption as the plasma beta approaches the Troyon limit. Time dependent studies for this case show that the region above ignition is accessible and stable up to the Murakami density limit, at which point maximum power output is achieved.

In the case of a disruptive or 'hard' beta limit, regions of density-temperature space where greater reactor power output is possible can be

reached by degrading confinement through various means such as ripple-induced losses, plasma size or current variation, or auxiliary power injection. Time evolution of plasma power balance show that the region of n-T space significantly above ignition is accessible using confinement degradation by auxiliary power, but very reliable active feedback control is required to maintain thermal stability.

Fractional power operation in the above scenarios is achieved by moving the operating point in (n-T) space. Once reaching the point of maximum power output, transitions to fractional power may be achieved by varying the ion fueling ratio, or decreasing the plasma current. A reactor with a divertor may operate between the L-mode and the H-mode, for the purpose of varying its operating point by changes in transport losses.

The reactor full power operating region and the strategies for fractional power operation vary considerably over the range of energy confinement scaling laws examined. The locus of n-T points defining the ignition curve and thus the accessible levels of reactor power also vary widely depending upon the confinement time scaling law. The dependence of confinement time on independently controlled parameters is still uncertain at this point.

For the more pessimistic scaling laws, in which confinement time is degraded by alpha heating power, an INTOR-sized tokamak will not ignite, whereas a high-field, high-density, compact tokamak is marginally likely to achieve ignition.

Those scaling laws which lead to optimistic ignition criteria pose the greatest problems in terms of burn control, because the desired operating region is well above the ignition curve in the thermally unstable operating regime. It is also found that neoclassical ion transport ($\tau_i/\tau_e > 1$) leads to very optimistic ignition condition when compared to anomalous ion losses for the same global transport losses.

Thermally stable operation of an ignited tokamak is identified for the following cases:

1. The reactor is operated marginally ignited with the ion fuel source and auxiliary power synchronized to an active feedback system.
2. A 'soft' beta limit applies.
3. An appropriately small fraction of alpha power degrades confinement time.
4. For the case in which auxiliary power degrades confinement, the region well above ignition is accessible and actively stable with auxiliary power feedback.
5. Confinement time degrades with plasma temperature rather than with input power.
6. Confinement scaling of the form $(a + b/P_{TOT})$ applies, as extrapolated from Doublet III results.

Maintaining thermal equilibrium while varying the reactor power output is generally synonymous with moving the ignition curve in (n-T) space, or moving along the ignition curve, so that the operating point in n-T space is always marginally ignited. An exception may be the case of operating with a 'soft' beta limit above the ignition curve.

Several possible mechanisms were investigated to change the ignited operating point depending on the assumed scaling law. The primary mechanisms focus on changing the transport losses by varying plasma current, density, auxiliary power or fuel mixture ratio. Less well understood, but speculative, mechanisms for control include: changing the ion to electron transport loss ratio, varying the divertor confinement mode (H or L), varying the fraction of alpha power degrading confinement, or small variations in the plasma dimensions.

In conclusion, we have shown that requirements for ignition and

fractional power operation are very sensitive to the assumed energy confinement scaling and especially to the effect of alpha power on confinement time. This underscores the need for an ignition experiment to study burn plasma physics in order to achieve realistic extrapolation to reactor-relevant confinement. Once ignition is achieved, maintaining thermal stability is not a trivial problem and will probably require active feedback systems. Feedback to the ion fuel source and the auxiliary power were found to be adequate for thermal stability, and thus sufficient to maintain reactor operation at fractions of rated power.

Acknowledgment

This work was performed under the auspices of U.S. Department of Energy Contract DE-AT03-80ER52061.

References

1) Houlberg, W.A., Attenberger, S.E.,Lao, L.L., "Computational Methods in Tokamak Transport," in Advances in Mathematical Methods for the Solution of Nuclear Engineering Problems, Proc. ANS/ENS International Topical Meeting, Munich, 1981, vol. 2.

2) Houlberg, W.A., Thermalization of an Energetic Heavy Ion in a Multispecies Plasma, FDM-103, Nuclear Engineering Dept., University of Wisconsin, Madison, Wisconsin, 1974.

3) Najmabadi, Farrohk, personal communication, June 1985.

4) Houlberg, W.A., Attenberger, S.E., Hively, L.M., Fusion Reactor Plasma Performance Modeling-Popcon Analysis, Nuc. Fus., 22, 935 (1982).

5) Conn, R.W., "Magnetic Fusion Reactors" in Fusion, ed., Teller, E., Academic Press, 1981.

6) Groebner, R.J. et al., "Experimentally Measured Ion-Thermal Conductivity Profiles in the Doublet-III Tokamak," GA Report #A17935, submitted to Nuclear Fusion (1985).

7) Mau, T.K., Conn, R.W., J. Fusion Energy, 2, 207 (1982).

8) (INTOR 83) - International Tokamak Reactor, Phase Two A, Part I, Report of the INTOR Workshop, EAEA, Vienna, 1983 (vol. I).

9) Rosenbluth, M.N., Hazeltime, R., Hinton, F.L., Phys. Fluids 15, 116 (1972), and Hinton, F.L., Hazeltime, R., Rev. Mod. Phys., 48, 239 (1976).

10) Potok, R.E., Bromberg, L., LeClaire, S., Physics and Engineering Tradeoffs in Tokamak Reactor Beta Scaling, presented at APS, Plasma Physics Division, San Diego, California, 1985.

11) (INTOR - USA '85) - U.S. Contribution to the International Tokamak Reactor, Phase Two A, Part 2, 1983-1985, Georgia Inst. of Tech., Atlanta, Georgia, July, 1985.

12) Troyon, F., et al., Plasma Phys. Controlled Fus., 26, 209 (1984).

13) Bernard, C., (see INTOR - USA '85).

14) Murakami, M., et al., Nucl. Fusion, 16, 347 (1976).

15) Kaye, S.M., Goldston, R.S., Global Energy Confinement Scaling for Neutral-Beam-Heated Tokamaks, Nucl. Fusion 25, 1 p.65 (1985).

16) Ejima, S., Bures, M., Christiansen, J.P., Cordey, et al., Energy Confinement Scaling of Ohmic and ICRF Heated JET Plasmas, presented at the APS, Plasma Physics Div., San Diego, 1985.

17) Merezhkin, V.G., Mukhovatov, V.S., JETP Lett. 33, p. 446 (1981).

18) Goldston, R.J., Energy Confinement Scaling in Tokamaks, Plasma Phys. Contr. Fus. 26, 87 (1984).

19) Ohkawa, T., "Energy Confinement Time of Tokamak Plasma with Auxiliary Heating," Comments Plasma Phys. Contr. Fus. 9, 127 (1985).

20) Kaye, S.M., Assessment of Energy Confinement Transport, and Scaling Results in Auxiliary Heated Tokamaks, PPPL-2217, Princeton Plasma Physics Lab, 1985, see also ref. 21.

21) Deboo, J., "Confinement Time Scaling for D-III," included in INTOR Phase II-A Data Base and R&D Needs Assessment, available at Princton Plasma Physics Lab, 1985.

22) Ohkawa, T., Comments Plasma Phys. Contr. Fus. 9, (1985).

23) Houlberg, W.A., "Transport Studies of Compact Tokamak Ignition Experiments," invited paper, APS Plasma Physics Div. Mtg., San Diego, 1985.

24) Uckan, N.A., Sheffield, J., "A Simple Procedure for Establishing Ignition Conditions in Tokamaks," ORNL/TM-9722, Oak Ridge National Lab, Oak Ridge, Tennessee, 1985.

25) Baker, et al., Starfire, ANL/FPP-80-1, Argonne National Lab, Argonne, Illinois, 1980.

26) Stacy, M.S., Jr., Fusion, Wiley-Interscience, New York, 1984.

27) Wagner, F., et al., Phys. Rev. Lett. 49, 1408 (1982) and in Proceedings of Plasma Physics and Cont. Fusion, vol. I, Baltimore, 1982, IAEA, Vienna, 1983.

28) Burrell, K.H., et al., in Cont. Fus. and Plasma Physics (Proc. 11th Europ. Conf., Aachen, 1983, vol.7D, pt. 1, 11 (1983).

29) Kaye, S.M., et al., J. Nucl. Mater. 121, 115 (1984).

Table I:
BASIC DEVICE PARAMETERS

	INTOR/UCLA	IGNITOR*	BRAND-X*
MAJOR RADIUS (M), R	5.3	1.0125	1.40
MINOR RADIUS (M), a	1.2	0.3875	0.50
TOROIDAL FIELD, B_o(T) (ON AXIS)	5.5	12.6	10.0
STEADY STATE CURRENT (MA)	6.4	10.0	10.0
ELONGATION, K	1.6	1.67	1.8
CYLINDRICAL SAFETY FACTOR, Q	2.1	2.0	2.0
CRITICAL BETA (%)	3.5	6.0	6.0
MAXIMUM DENSITY ($10^{20}m^{-3}$)	1.5	9.3	5.4
THERMAL CYCLE EFFICIENCY, η_{TH}	0.35		
AUXILIARY POWER SYSTEM EFFICIENCY, η_{AUX}	0.55		
OHMIC POWER EFFICIENCY, η_{OH}	0.95		
ADDITIONAL BASE-LINE POWER REQUIREMENTS, P_{BAS}	150 MW		
BLANKET MULTIPLICATION, M	1.2		

* (Values from Reference 23)

Table II: Confinement Scaling Laws

Scaling	Equation for τ(s)	Reference
Intor/Alcator	$\tau = 5\times10^{-21} n_e(m^{-3}) a^2(m)$	8
Mereshkin	$\tau = 3.5\times10^{-21} \cdot (a/R)^{0.25} \cdot q \cdot n_e(cm^{-3}) \cdot R^3(cm) \bar{T}_e^{-0.5}(KeV)$	17
Goldston	$\tau = (1./\tau_{aux}^2 + 1./\tau_{ohm}^2)^{-0.5}$	18
	where: $\tau_{aux} = 6.4\times10^{-8} \cdot I_p(A) \cdot K^{0.5} \cdot a^{-.37}(cm) R^{1.75}(cm) P_{IN}^{-0.5}(W)$	
	and: $\tau_{ohm} = 7.1\times10^{-22} \cdot n_e(cm^{-3}) \cdot a^{1.04}(cm) R^{2.04}(cm) q^{0.5}$	
Ohkawa	$\tau = 1.\times10^{-20} \cdot n_e(cm^{-3}) \cdot a(cm) \cdot R^2(cm) \cdot q \cdot T_e^{-0.5}(KeV)(1+P_{IN}/P_{ohm})^{-0.5}$	19
Kaye-Goldston	$\tau=10.^{-2.56} \cdot n_e^{0.26}(10^{19} m^{-3}) \cdot a^{-.49}(cm) \cdot R^{1.65}(cm) \cdot K^{0.28} \cdot I_p^{1.24}(KA) \cdot B_o^{-.09}(T) \cdot P_{IN}^{-0.58}(MW)$	15
Doublet III:	for: $C_d=(a^2(m)/0.41^2) \cdot I_p(MA) \cdot K^{0.5}$	21
limiter 1	$\tau=C_d \cdot (0.074 \cdot P_{IN}^{-0.46}(MW))$	
limiter 2	$\tau = C_d \cdot (0.025 + 0.058/P_{IN}(MW))$	
divertor 1	$\tau = C_d \cdot (0.114 \cdot P_{IN}^{-0.34})$	
divertor 2	$\tau = C_d \cdot (0.058 + 0.061/P_{IN}(MW))$	

where:
- q = cylindrical edge safety factor
- K = plasma elongation
- I_p = plasma steady state toroidal current
- P_{IN} = plasma injected heating power
- $P_{IN} = f_{aux} \cdot P_{aux} + f_\alpha \cdot P_\alpha$

where f_{aux} = a specified fraction of the auxiliary power, P_{aux}, and f_α = a specified fraction of the alpha fusion power, P_α.

Listing of Figures and Captions

Fig. 1. Ignition contours ($P_{aux} = 0$) for several of the energy confinement time scaling laws shown in Table II.

Fig. 2. Ignition contours for the Doublet III scaling laws, L = Limiter, D = divertor, 1: $\tau \sim a \cdot P_{IN}^{-b}$, 2: $\tau \sim a + b/P_{IN}$, AUX: $P_{IN} = P_{AUX}$, α: $P_{IN} = P_{AUX} + P_{\alpha}$.

Fig. 3.(a,b) Simple ignition power balance for Goldston (3a) and for Kaye-Goldston (3b) scalings assuming that $P_{IN} = P_{\alpha}$.

Fig. 4. Temperature versus time for cases varying the fraction of fusion alpha power that degrades confinement time. (Goldston scaling).

Fig. 5. Ignition curves for varying (τ_{Ei}/τ_{Ee}), the ratio of ion energy confinement time to that for the electrons.

Fig. 6. Ignition curves for confinement times with constant values. Shaded areas indicate ignited regions for each ignition curve which can be made marginally ignited by decreasing confinement time by 10%.

Fig. 7. Equilibrium power contours for the Goldston scaling, ohmic tau term only. Negative values are in the ignited region and indicate the amount of power that must be removed from the plasma to stay at that point in thermal equilibrium.

Fig. 8. Maximum auxiliary power required for specified constant values of confinement time for an INTOR sized tokamak.

Fig. 9.(a-d) Auxiliary power surfaces for 4 cases, 1) Goldston, ohmic only, 2) Goldston scaling with $\tau_i/\tau_e = 1.5$, 3) Goldston scaling with $\tau_i = 1.1 \times \tau_e$, and 4) Kaye-Goldston scaling $(\tau_i/\tau_e = 1.5)$.

Also included are the corresponding surfaces of reactor net electric power to indicate the regions of (n-T) space for desired operations.

Fig. 10. Contours of select key parameters in reactor design. The beta limit (3.5% in this case), the net electric power contours of $P_{net} = 0$ and $P_{net} = 250$ (a practical maximum for this case) are shown with three different possible ignition curves.

Fig. 11. Density-temperature trajectory for the "soft-beta" case.

Fig. 12.(a-f) Time dependence of several plasma and operating parameters during the trajectory shown in Fig. 11. (Note: Net electron power does not include the 150 MW base line power.)

Fig. 13. Density-temperature trajectory for simple feedback scheme showing unstable operating point leading to thermal runaway (Goldston ohmic-only scaling).

Fig. 14. Density-temperature trajectory for feedback scheme maintaining plasma at marginally subignited densities, and reaching equilibrium. (Goldston ohmic-only scaling).

Fig. 15.(a-g) Time dependence of several plasma and operating parameters during the trajectory shown in Fig. 14. (Note: Net electron power does not include the 150 MW base line power.)

Fig. 16. Density-temperature trajectory using auxiliary power to degrade confinement and thus maintain thermal stability in the ignited region (Goldston scaling).

Fig. 17.(a-g) Time dependence of several plasma and operating parameters during the trajectory shown in Fig. 16. (Note: Net electron power does not include the 150 MW base line power.)

Fig. 18. Temperature versus time for cases of different constant density (Ohkawa scaling - ohmic term only).

Fig. 19. Temperature versus time for cases of different f_D, the deuterium fraction of the ion fuel, at constant average density of 1.1 ($10^{20}m^{-3}$). The time dependence of the ohmic power and the auxiliary power curves are superimposed in a qualitative manner. Ignition is at t ~ 20 sec. (Ohkawa scaling, ohmic term only).

Fig. 20. Operating point trajectories in (n-T) space for two cases superimposed on the net electric power contours. The Goldston (ohmic-only) scaling ignition curve and two beta value contours are also shown.

Fig. 21. Operating point trajectories in (n-T) space superimposed on the net electric power contours for the case of an ignition curve with marginal thermal stability. (Ohkawa scaling, ohmic term only).

Fig. 22. Operating point trajectories in (n-T) space superimposed on net electric power contours for the cases of more desirable ignition curves (...,3). This also includes a trajectory, C, for the desirable "soft-beta" case.

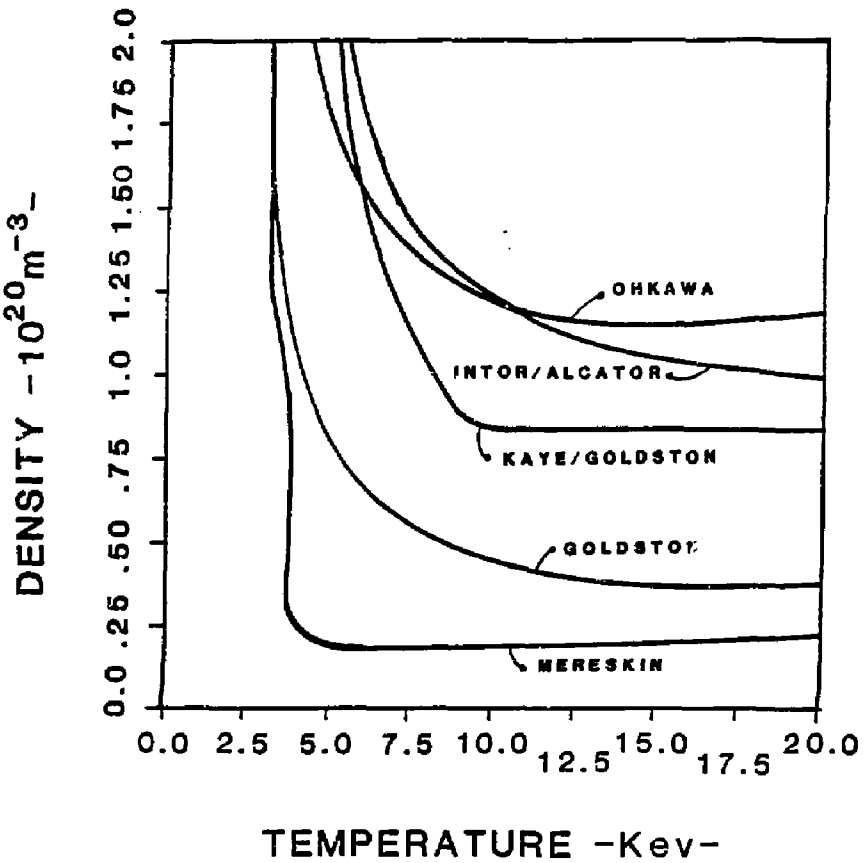
DENSITY -$10^{20}m^{-3}$-
0.0 .25 .50 .75 1.0 1.25 1.50 1.75 2.0
0.0 2.5 5.0 7.5 10.0 12.5 15.0 17.5 20.0
TEMPERATURE -Kev-
OHKAWA
INTOR/ALCATOR
KAYE/GOLDSTON
GOLDSTON
MERESKIN

Figure 1

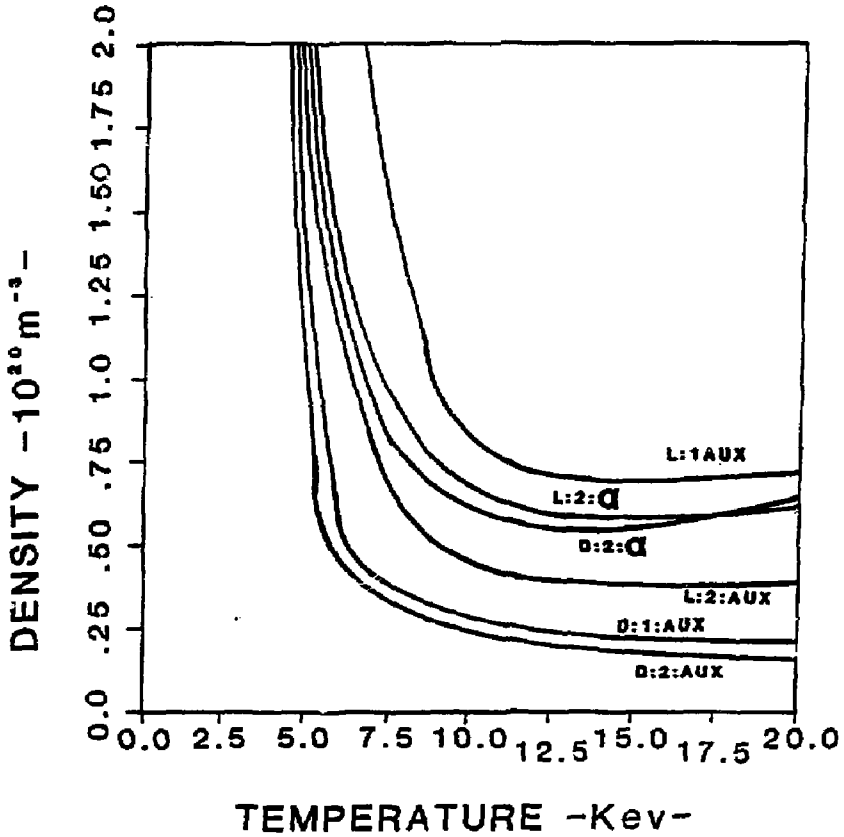
DENSITY -10²⁰m⁻³-
0.0 .25 .50 .75 1.0 1.25 1.50 1.75 2.0
0.0 2.5 5.0 7.5 10.0 12.5 15.0 17.5 20.0
TEMPERATURE -Kev-
L:1AUX
L:2:α
D:2:α
L:2:AUX
D:1:AUX
D:2:AUX

Figure 2

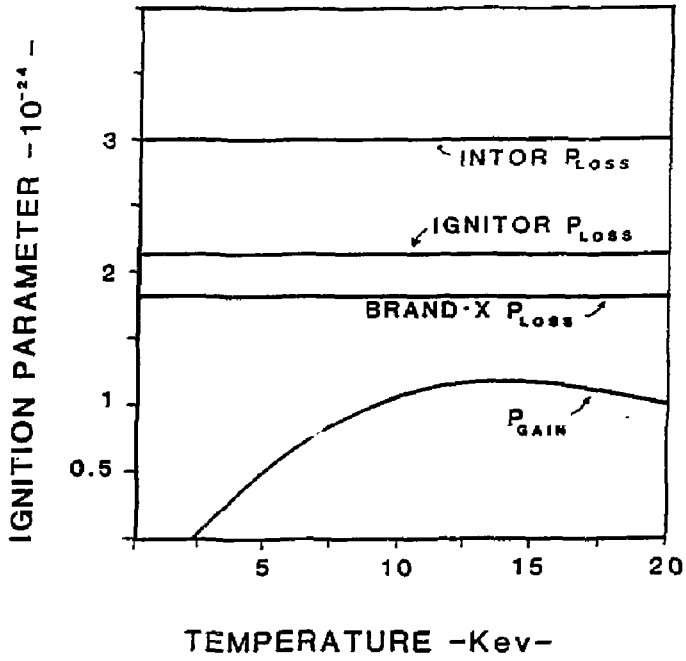
IGNITION PARAMETER -10⁻²⁴-
3
2
1
0.5
INTOR P_LOSS
IGNITOR P_LOSS
BRAND-X P_LOSS
P_GAIN
5
10
15
20
TEMPERATURE -Kev-

a

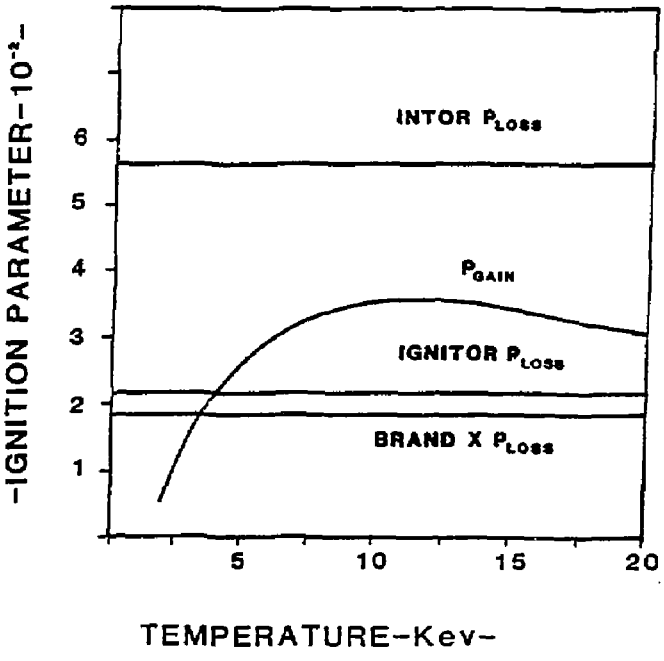
-IGNITION PARAMETER-10⁻²-
6
5
4
3
2
1
INTOR P_LOSS
P_GAIN
IGNITOR P_LOSS
BRAND X P_LOSS
5
10
15
20
TEMPERATURE-Kev-

b

Figure 3

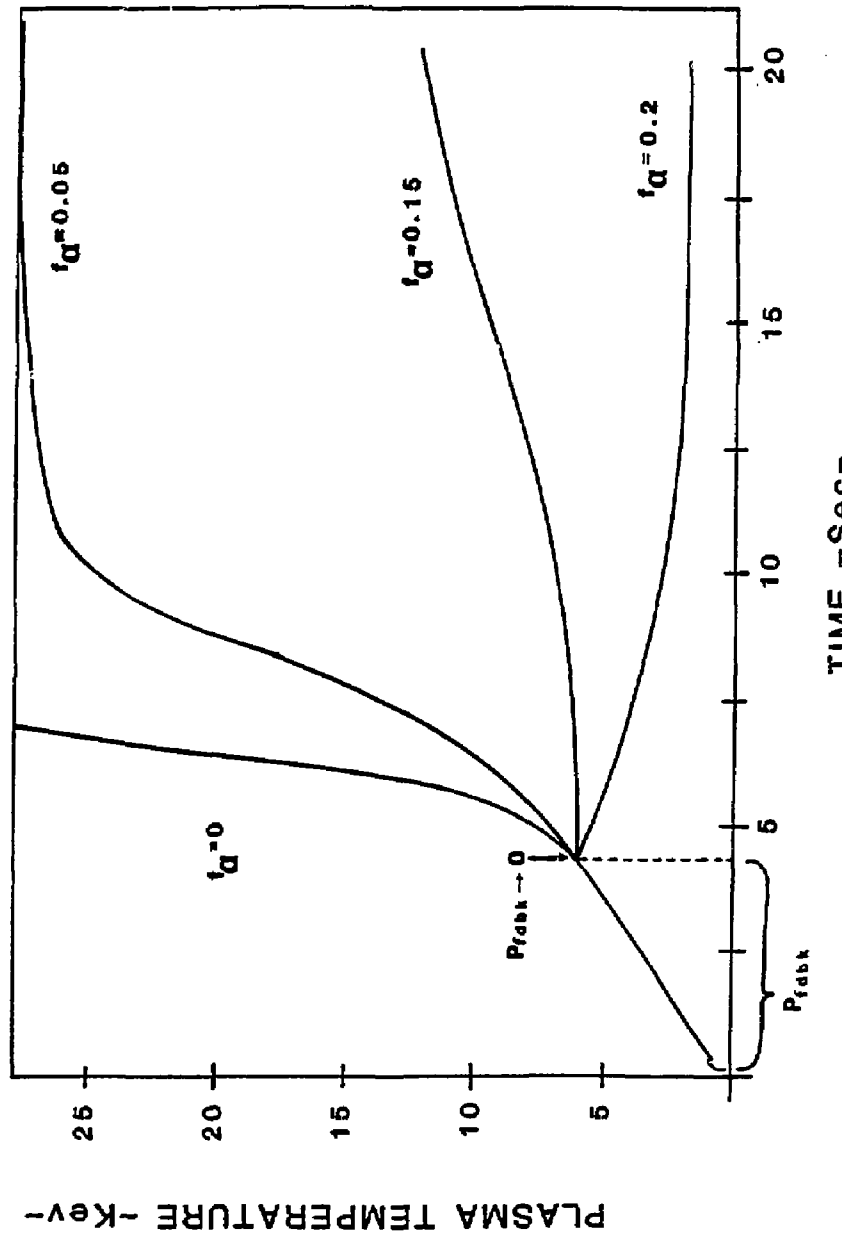
PLASMA TEMPERATURE -Kev-
TIME -Sec-
f_α=0.05
f_α=0.15
f_α=0.2
f_α=0
$P_{fdbk} \rightarrow 0$
P_{fdbk}
25
20
15
10
5
5
10
15
20

Figure 4

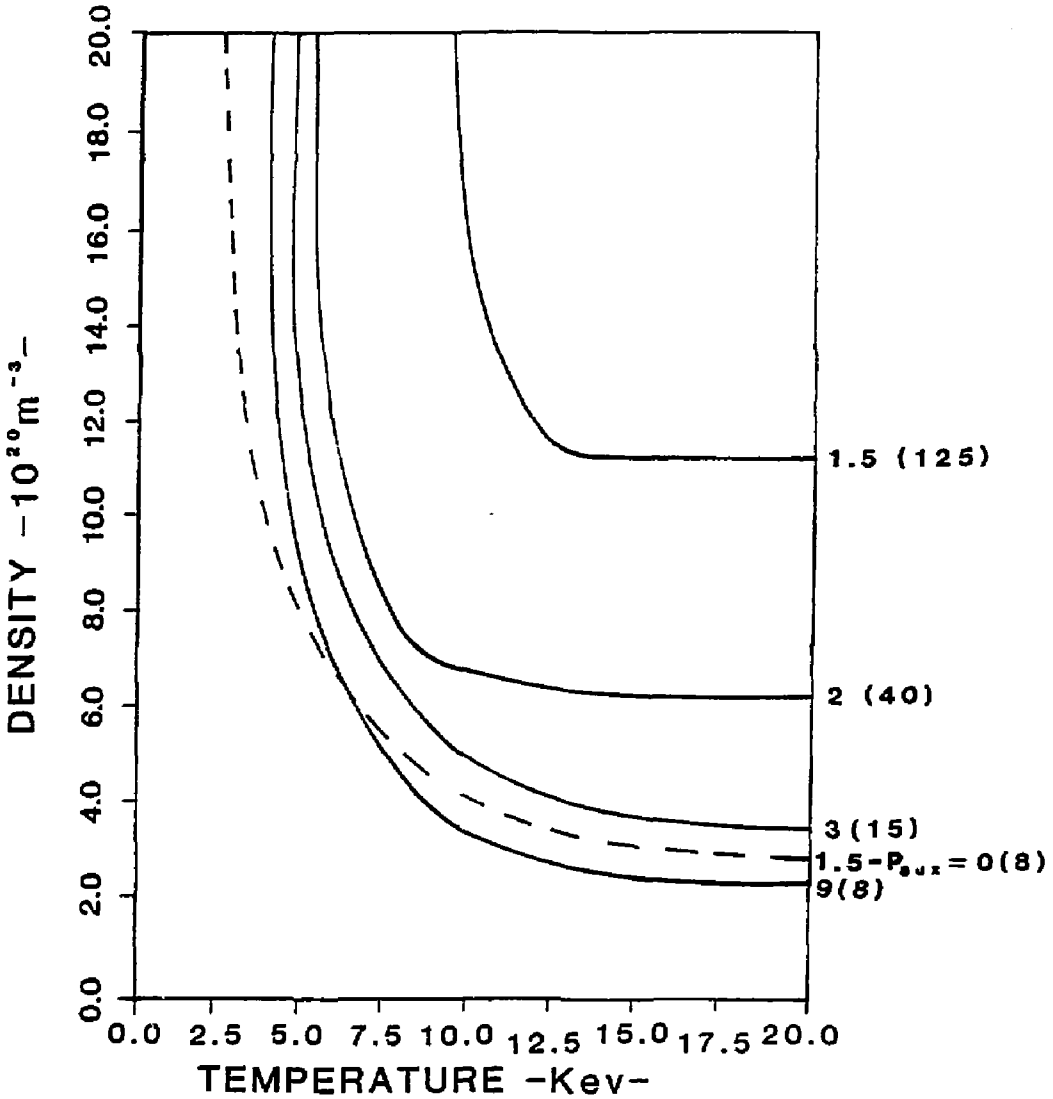
DENSITY -$10^{20}m^{-3}$-
0.0
2.0
4.0
6.0
8.0
10.0
12.0
14.0
16.0
18.0
20.0
0.0 2.5 5.0 7.5 10.0 12.5 15.0 17.5 20.0
TEMPERATURE -Kev-
1.5 (125)
2 (40)
3 (15)
1.5-P_{aux} = 0(8)
9(8)

Figure 5

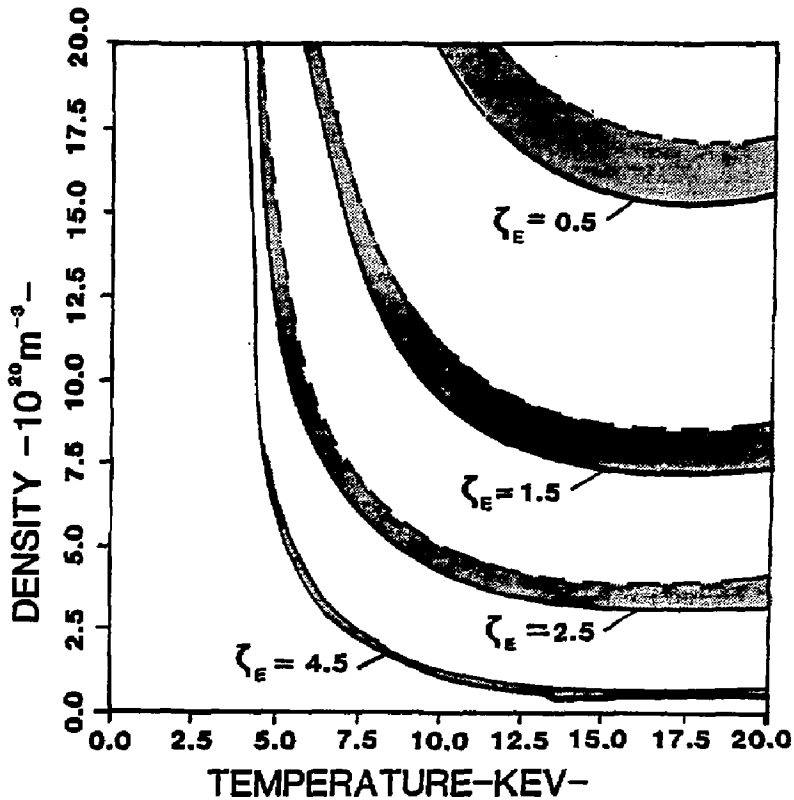
DENSITY -10^20 m^-3-
0.0
2.5
5.0
7.5
10.0
12.5
15.0
17.5
20.0
TEMPERATURE-KEV-
ζE = 0.5
ζE = 1.5
ζE = 2.5
ζE = 4.5

Figure 6

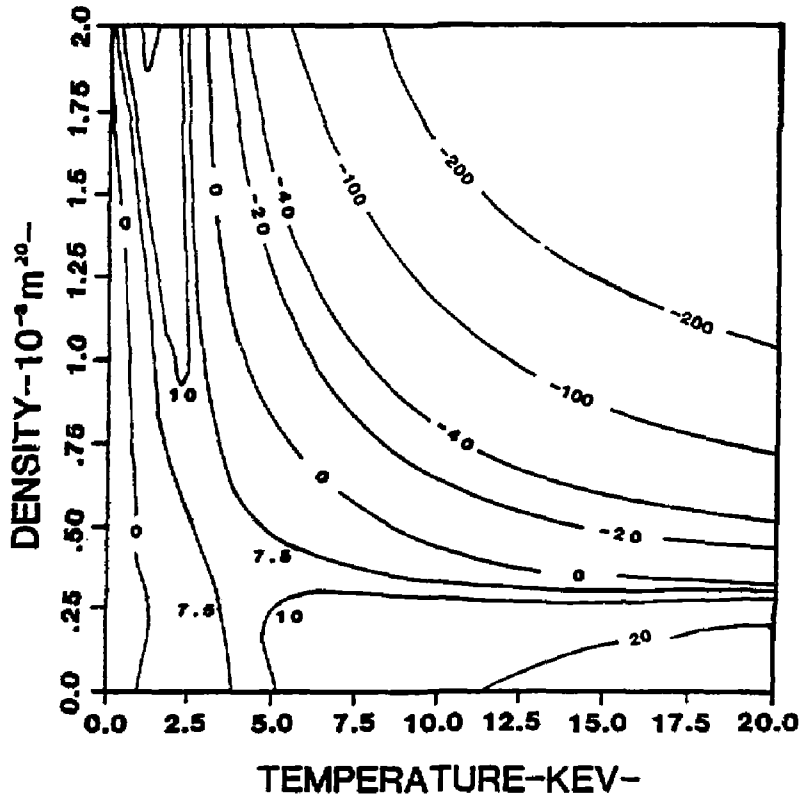
DENSITY--10⁻⁶m⁻³⁰-
2.0
1.75
1.5
1.25
1.0
.75
.50
.25
0.0
0.0
2.5
5.0
7.5
10.0
12.5
15.0
17.5
20.0
TEMPERATURE-KEV-
-200
-100
-40
-20
0
7.5
10
20

Figure 7

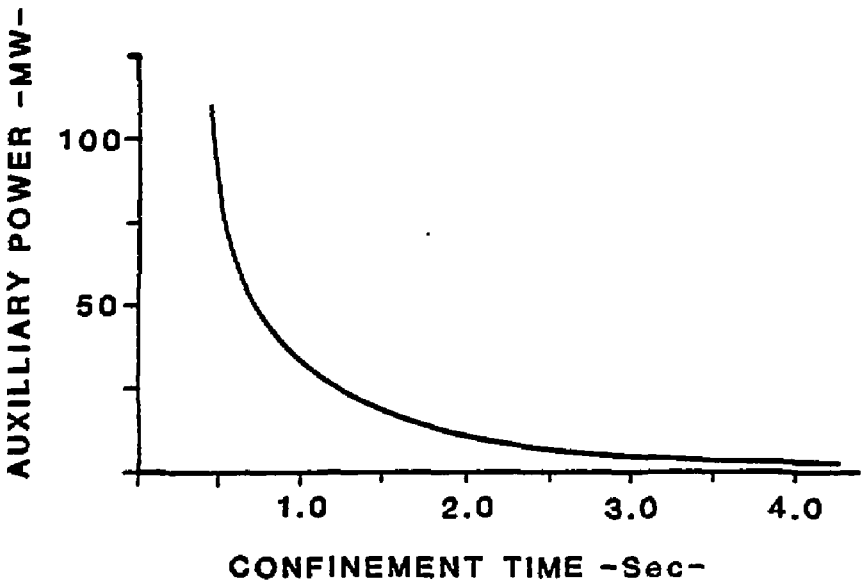

Figure 8

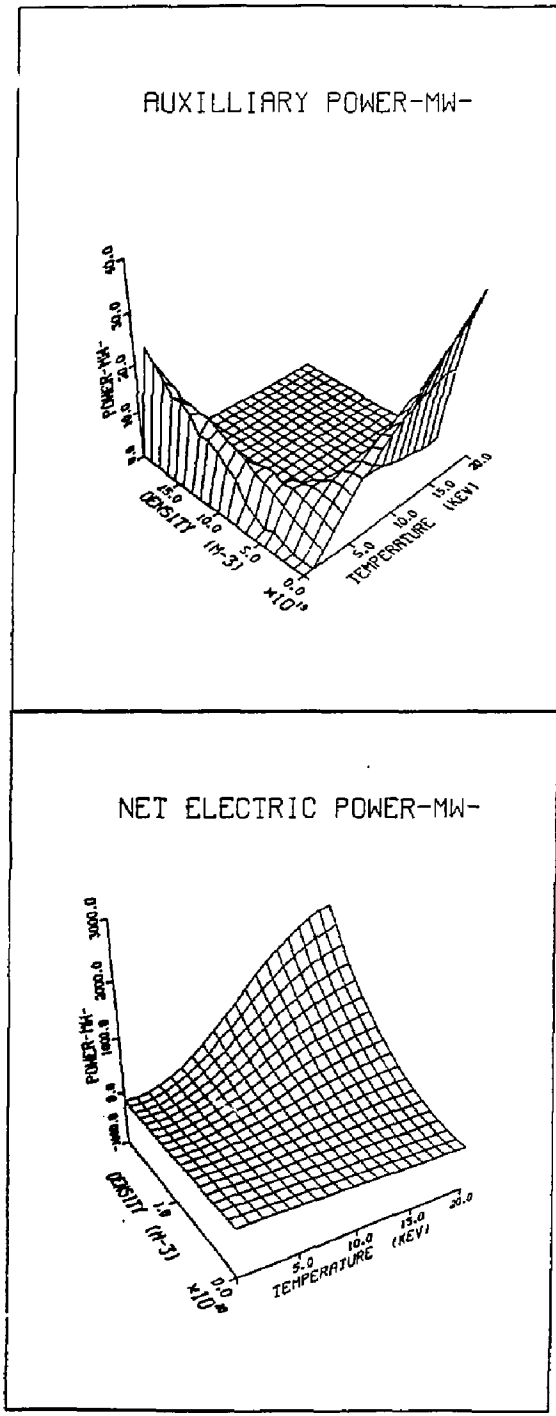
AUXILLIARY POWER-MW-
POWER-MW-
45.0
30.0
20.0
10.0
0.0
DENSITY (M-3)
15.0
10.0
5.0
0.0
X10^20
TEMPERATURE (KEV)
5.0
10.0
15.0
20.0
NET ELECTRIC POWER-MW-
POWER-MW-
3000.0
2000.0
1000.0
0.0
-1000.0
DENSITY (M-3)
1.0
0.0
X10^20
TEMPERATURE (KEV)
5.0
10.0
15.0
20.0

Figure 9a

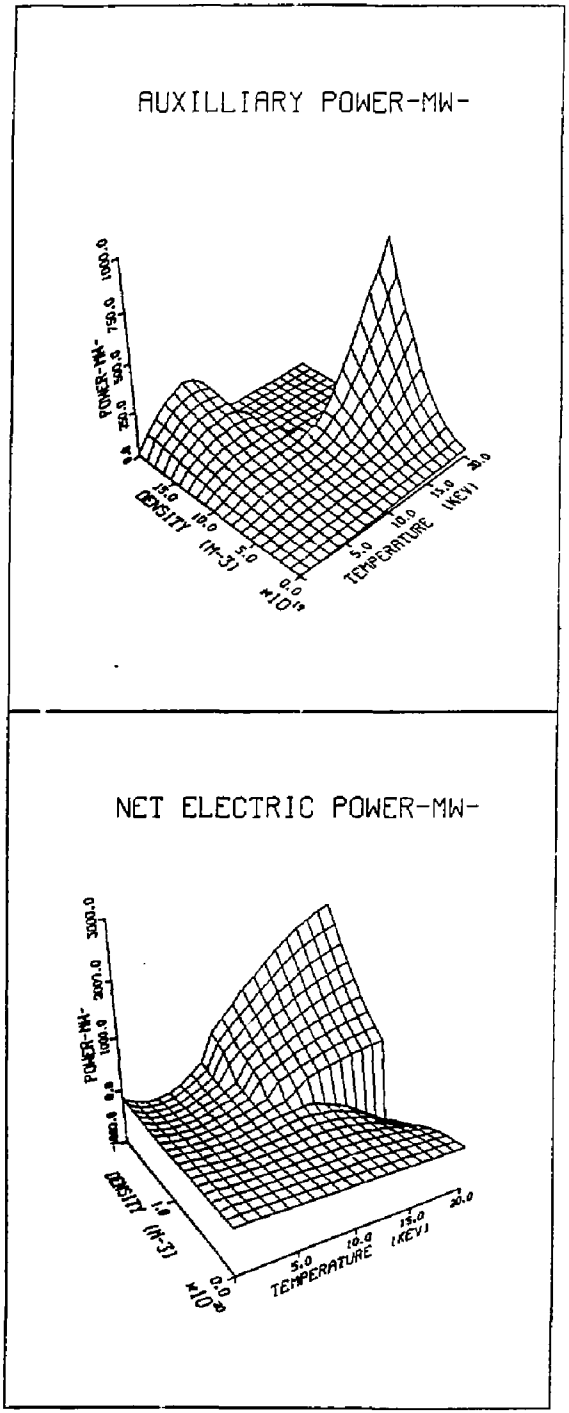
AUXILLIARY POWER-MW-
POWER-MW-
1000.0
750.0
500.0
250.0
0.0
DENSITY (M-3)
15.0
10.0
5.0
0.0
×10²⁰
TEMPERATURE
5.0
10.0
15.0
20.0
(KEV)
NET ELECTRIC POWER-MW-
POWER-MW-
3000.0
2500.0
2000.0
1500.0
1000.0
500.0
0.0
DENSITY (M-3)
1.0
0.0
×10²⁰
TEMPERATURE
5.0
10.0
15.0
20.0
(KEV)

Figure 9b

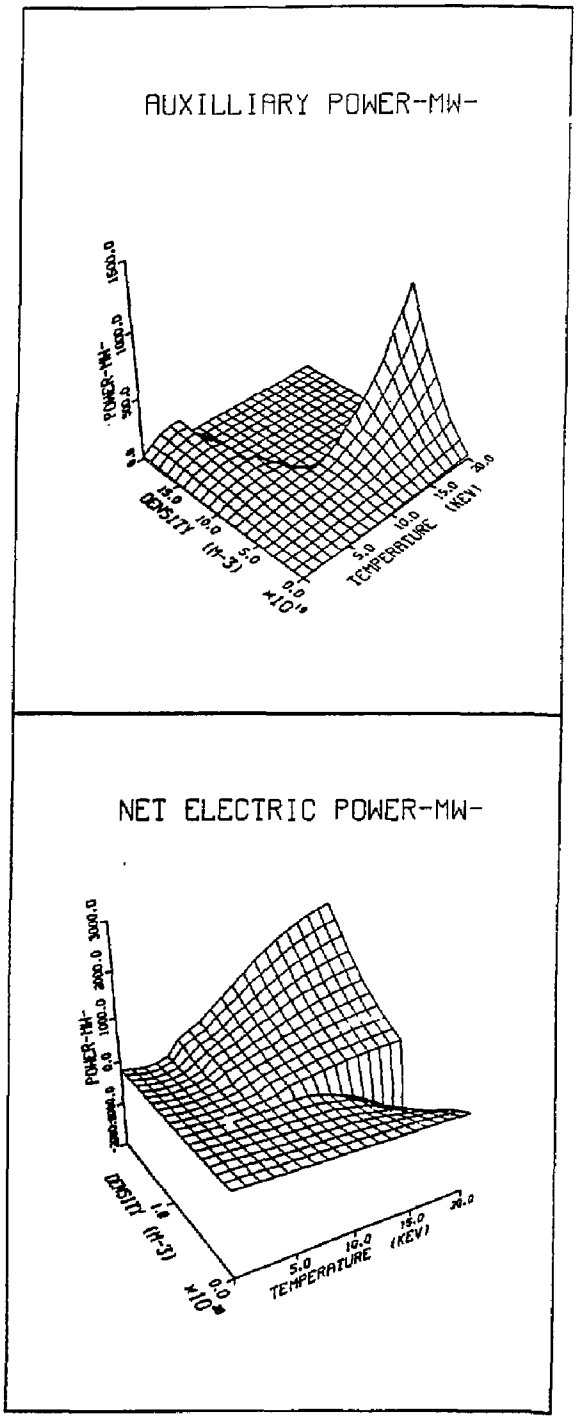
AUXILLIARY POWER-MW-
POWER-MW-
1500.0
1000.0
500.0
0.0
DENSITY
(M-3)
x10^20
TEMPERATURE
(KEV)
NET ELECTRIC POWER-MW-
POWER-MW-
3000.0
2000.0
1000.0
0.0
DENSITY
(M-3)
x10^20
TEMPERATURE
(KEV)

Figure 9c

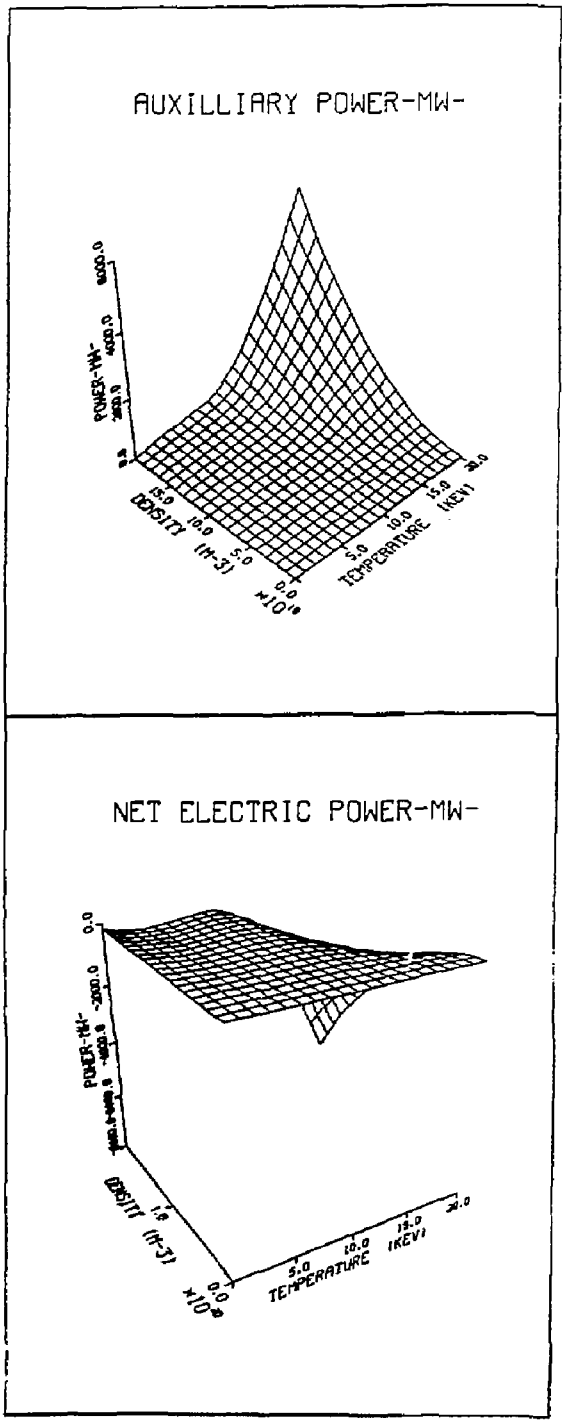
AUXILLIARY POWER-MW-
POWER-MW-
8000.0
4000.0
DENSITY (M-3)
TEMPERATURE (KEV)
NET ELECTRIC POWER-MW-
0.0
-2000.0
POWER-MW-
DENSITY (M-3)
TEMPERATURE
IKEV)

Figure 9d

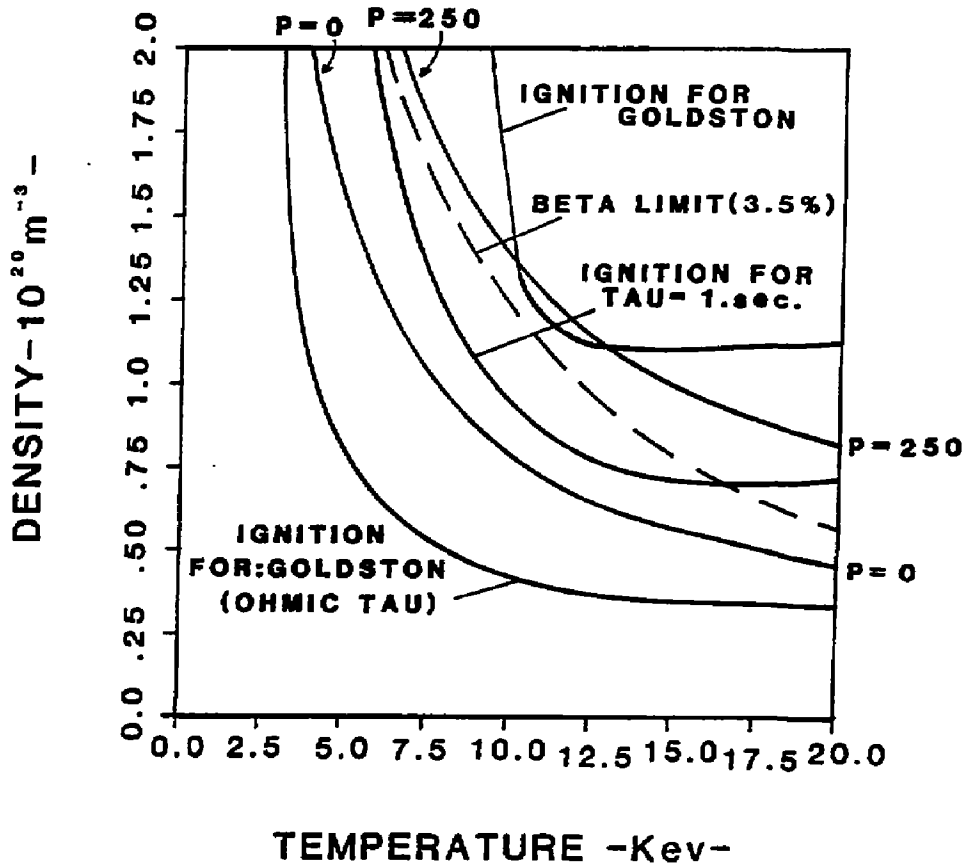
P=0
P=250
IGNITION FOR GOLDSTON
BETA LIMIT(3.5%)
IGNITION FOR TAU=1.sec.
P=250
P=0
IGNITION FOR:GOLDSTON (OHMIC TAU)
DENSITY-10^20 m^-3-
0.0 .25 .50 .75 1.0 1.25 1.5 1.75 2.0
0.0 2.5 5.0 7.5 10.0 12.5 15.0 17.5 20.0
TEMPERATURE -Kev-

Figure 10

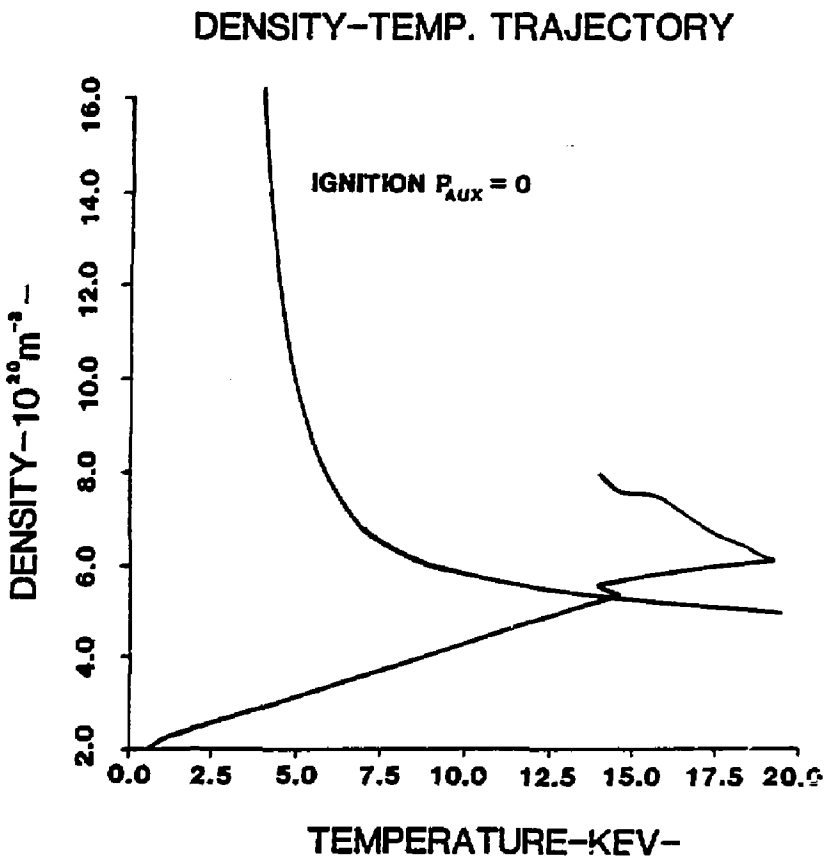
DENSITY-TEMP. TRAJECTORY
IGNITION $P_{AUX} = 0$
DENSITY-$10^{20}m^{-3}$-
2.0
4.0
6.0
8.0
10.0
12.0
14.0
16.0
0.0
2.5
5.0
7.5
10.0
12.5
15.0
17.5
20.0
TEMPERATURE-KEV-

Figure 11

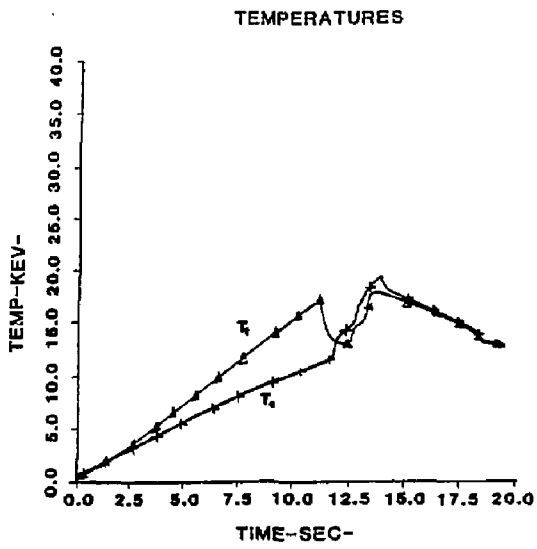

a

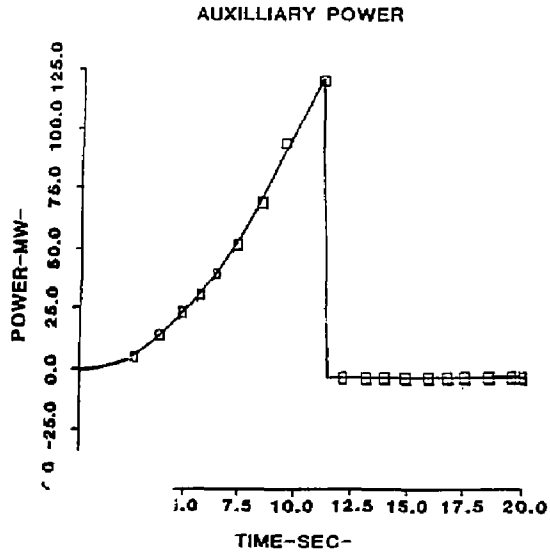

b

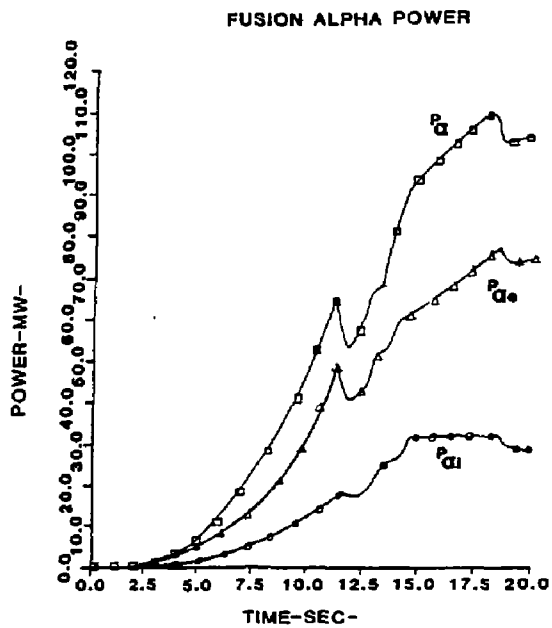

c

Figure 12 a-c

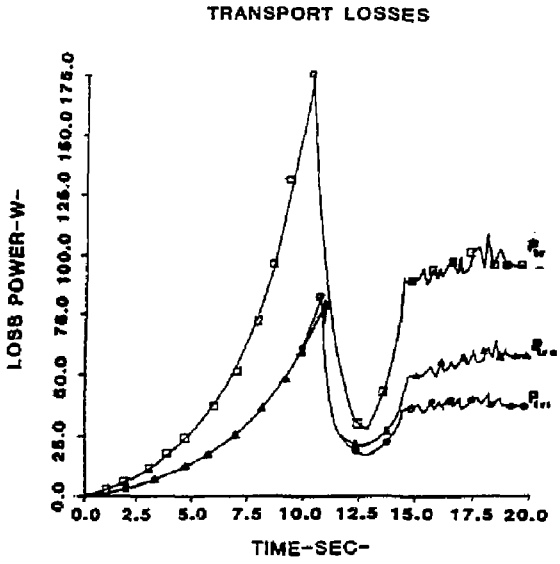

d

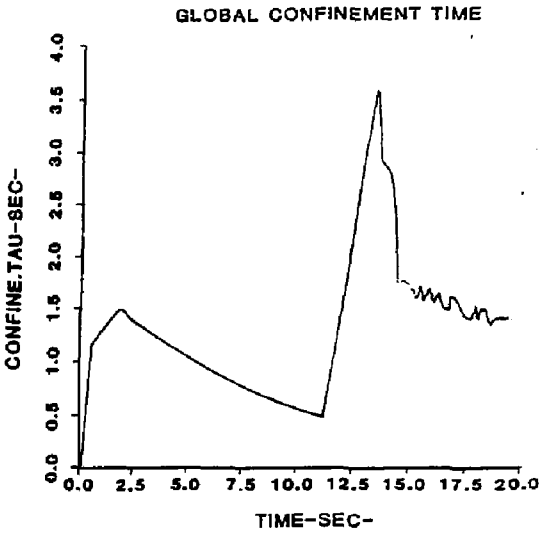

e

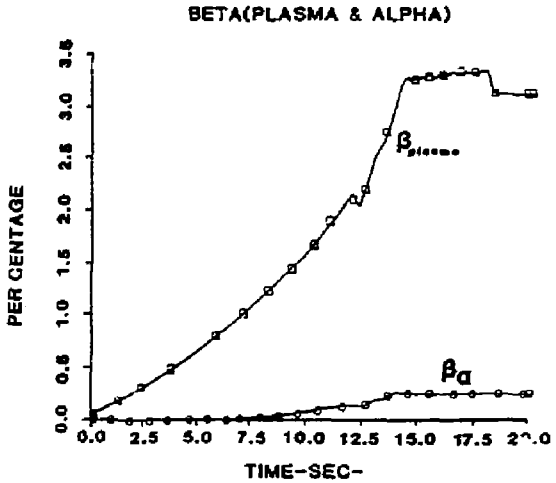

f

Figure 12 d-f

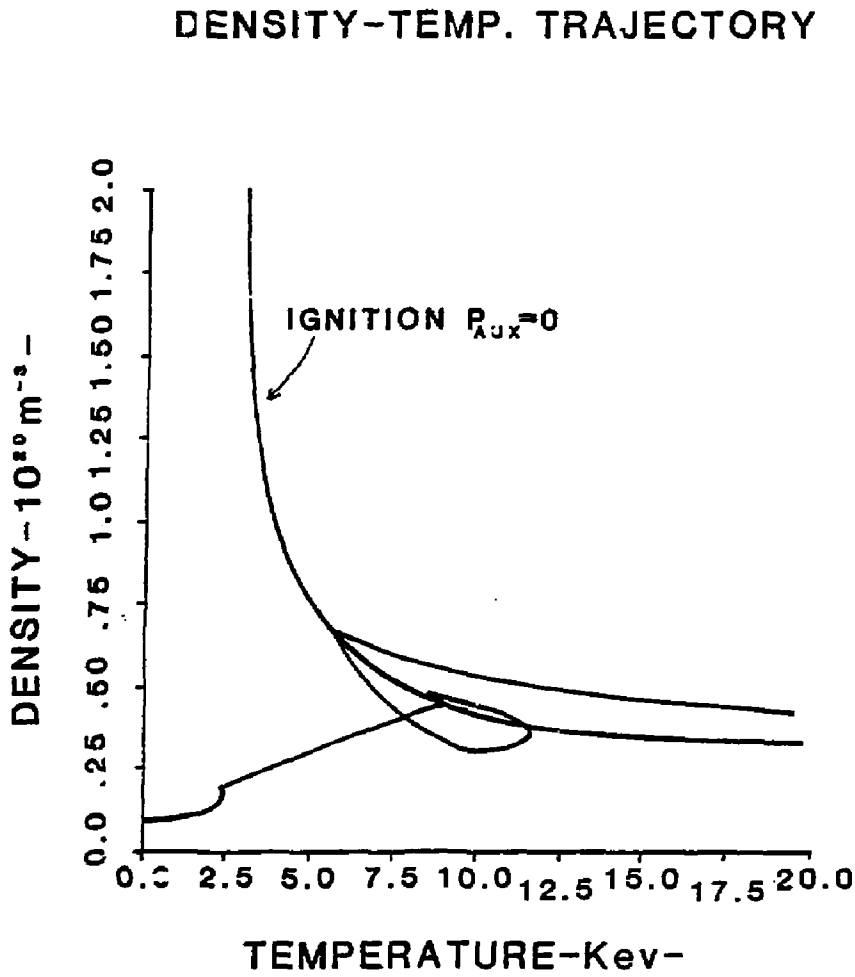
DENSITY-TEMP. TRAJECTORY
IGNITION $P_{AUX}=0$
DENSITY-10^{20} m^{-3}-
0.0 .25 .50 .75 1.0 1.25 1.50 1.75 2.0
0.0 2.5 5.0 7.5 10.0 12.5 15.0 17.5 20.0
TEMPERATURE-Kev-

Figure 13

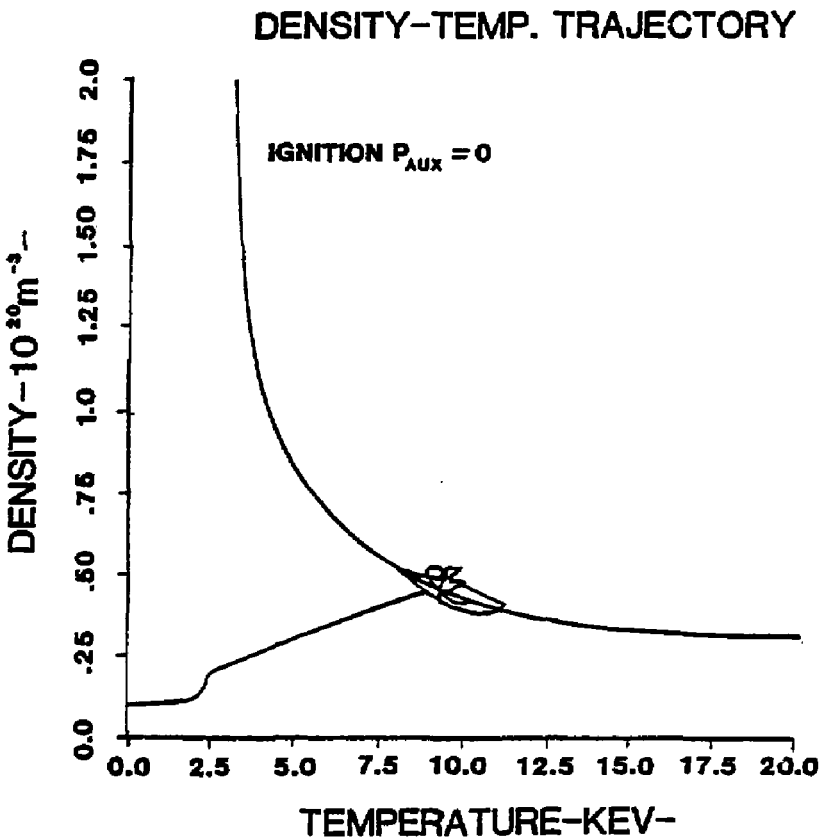
DENSITY-TEMP. TRAJECTORY
IGNITION $P_{AUX} = 0$
DENSITY-$10^{20}m^{-3}$-
0.0
.25
.50
.75
1.0
1.25
1.50
1.75
2.0
0.0
2.5
5.0
7.5
10.0
12.5
15.0
17.5
20.0
TEMPERATURE-KEV-

Figure 14

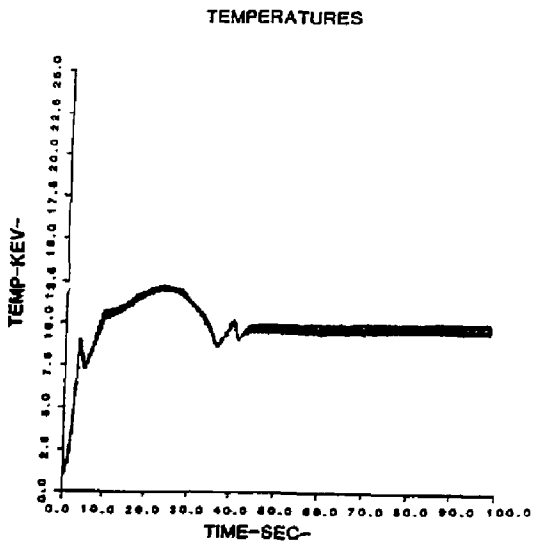

a

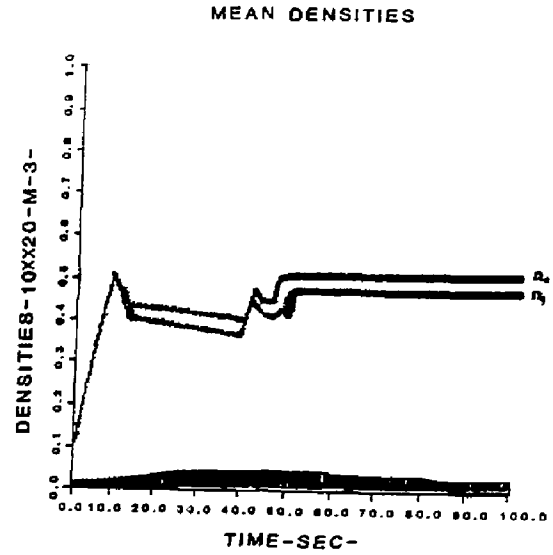

b

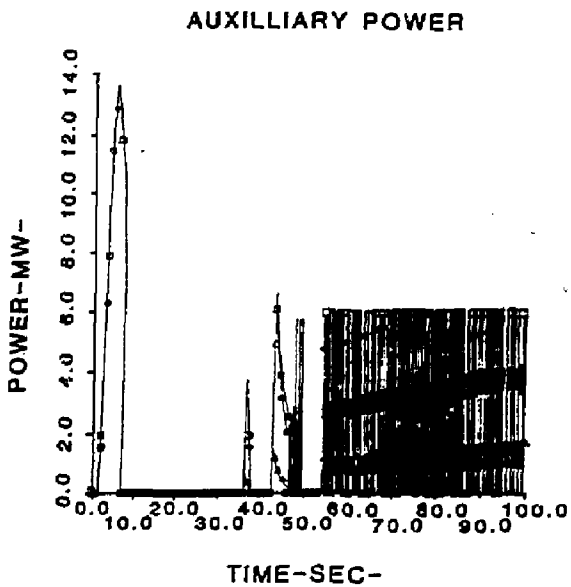

c

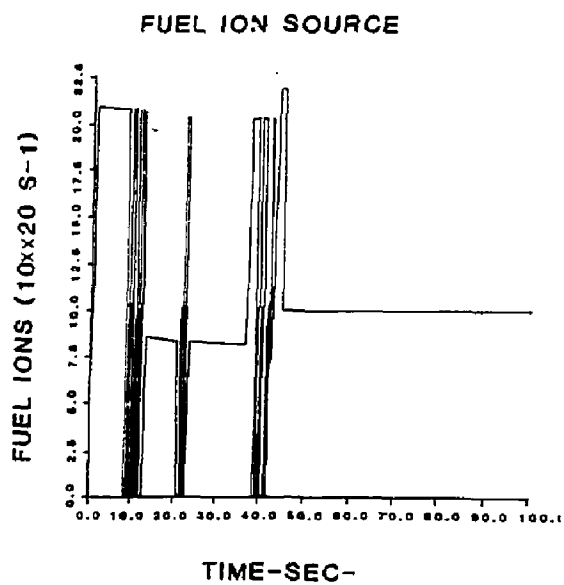

d

Figure 15 a-d

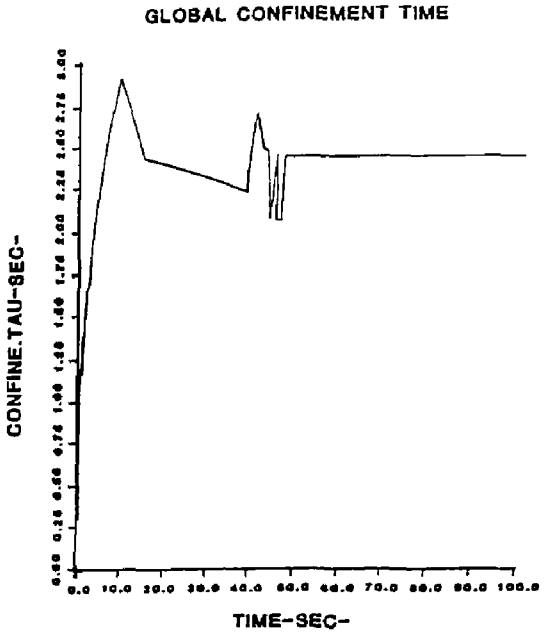

e

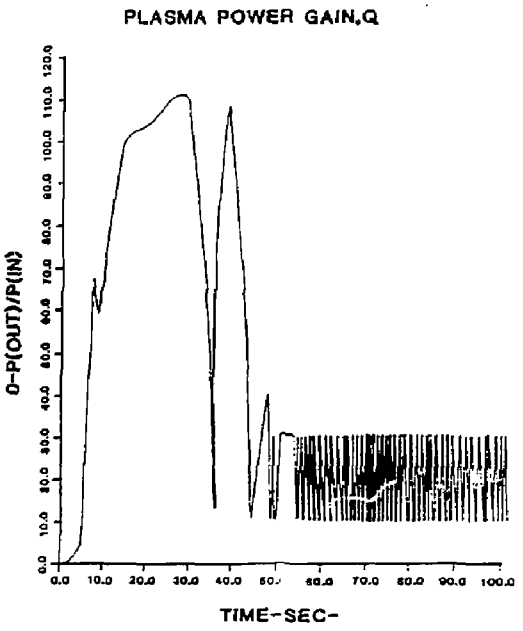

f

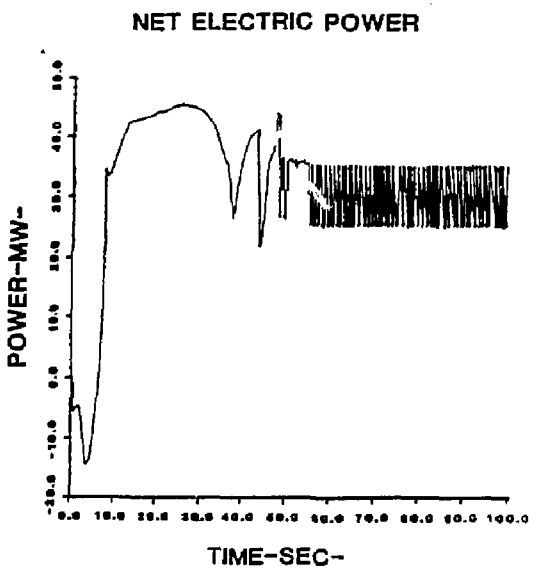

g

Figure 15 e-g

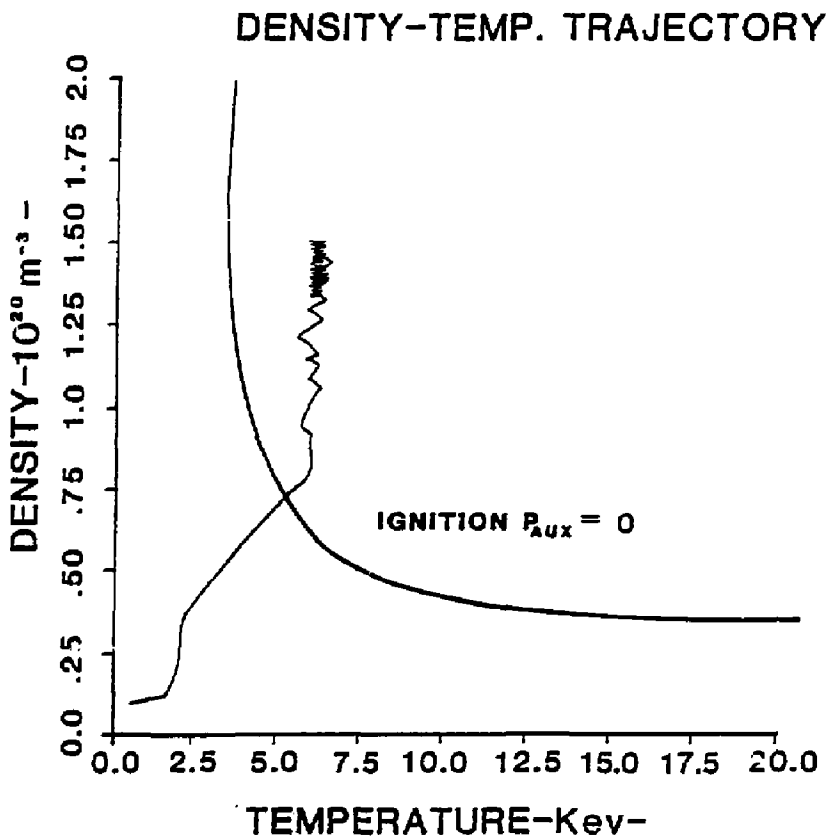
DENSITY-TEMP. TRAJECTORY
DENSITY-10²⁰ m⁻³ -
0.0 .25 .50 .75 1.0 1.25 1.50 1.75 2.0
IGNITION P_Aux = 0
0.0 2.5 5.0 7.5 10.0 12.5 15.0 17.5 20.0
TEMPERATURE-Kev-

Figure 16

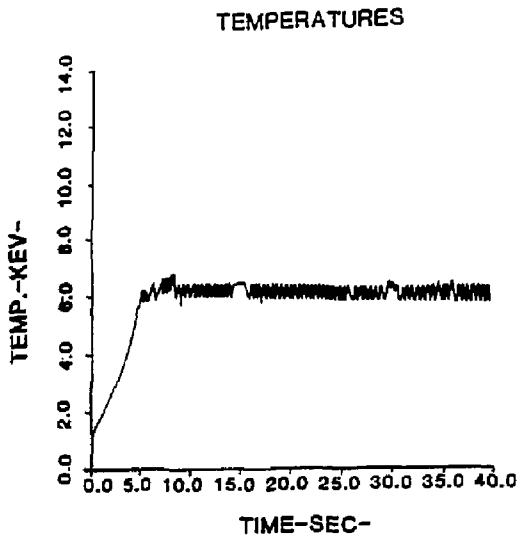

a

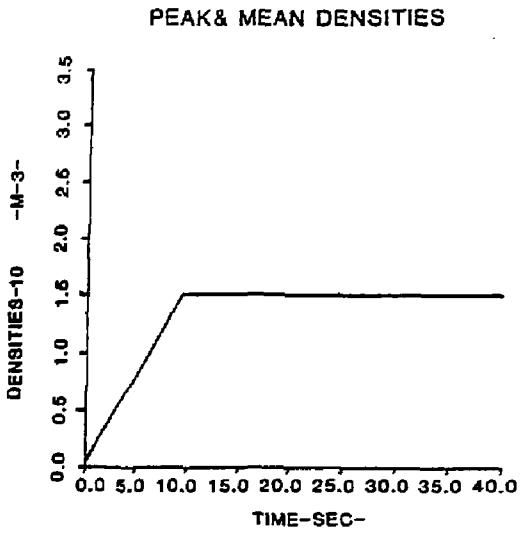

b

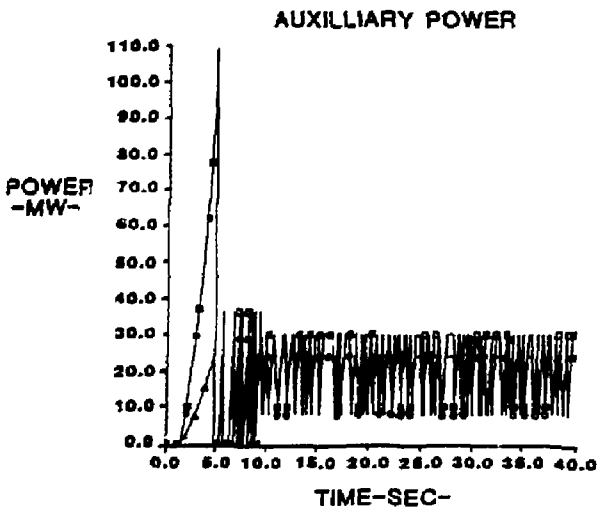

c

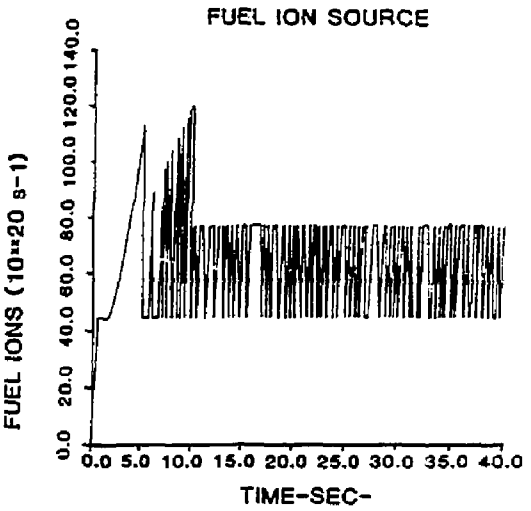

d

Figure 17 a-d

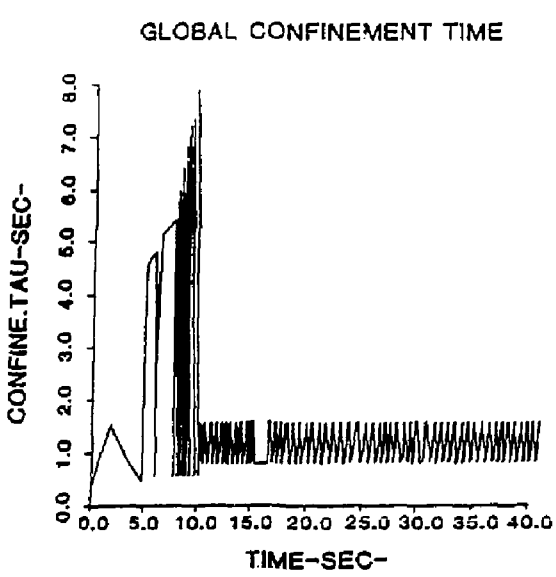

e

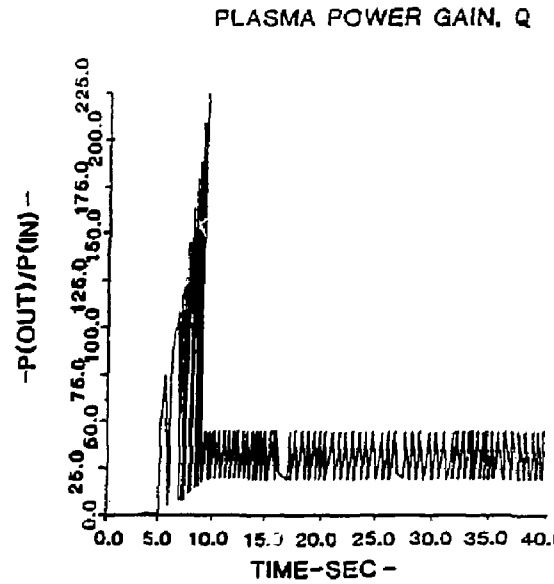

f

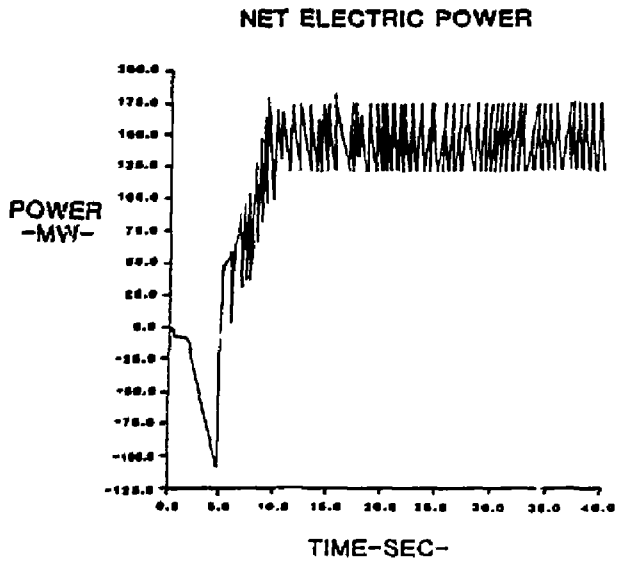

g

Figure 17 e-g

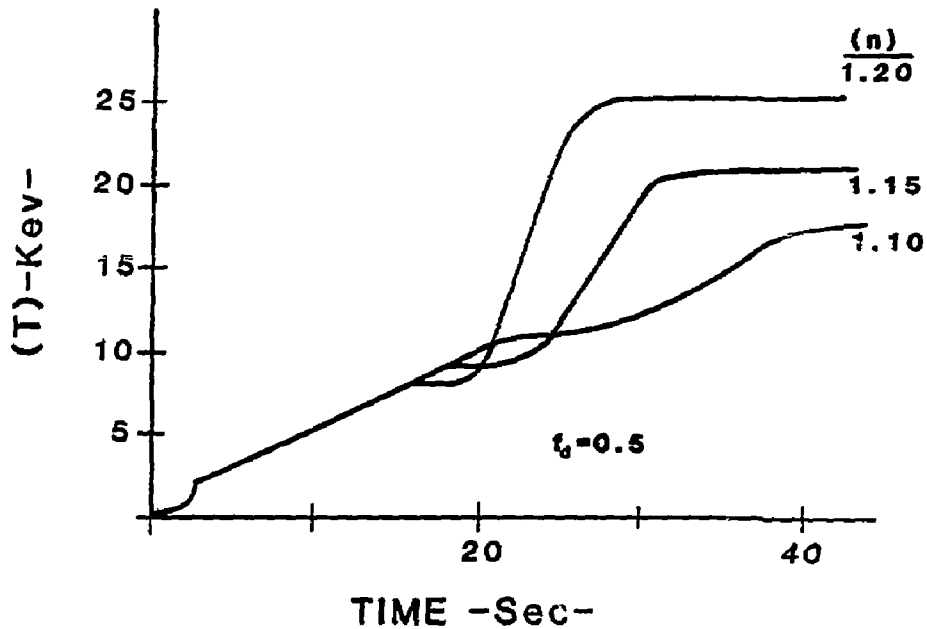

Figure 18

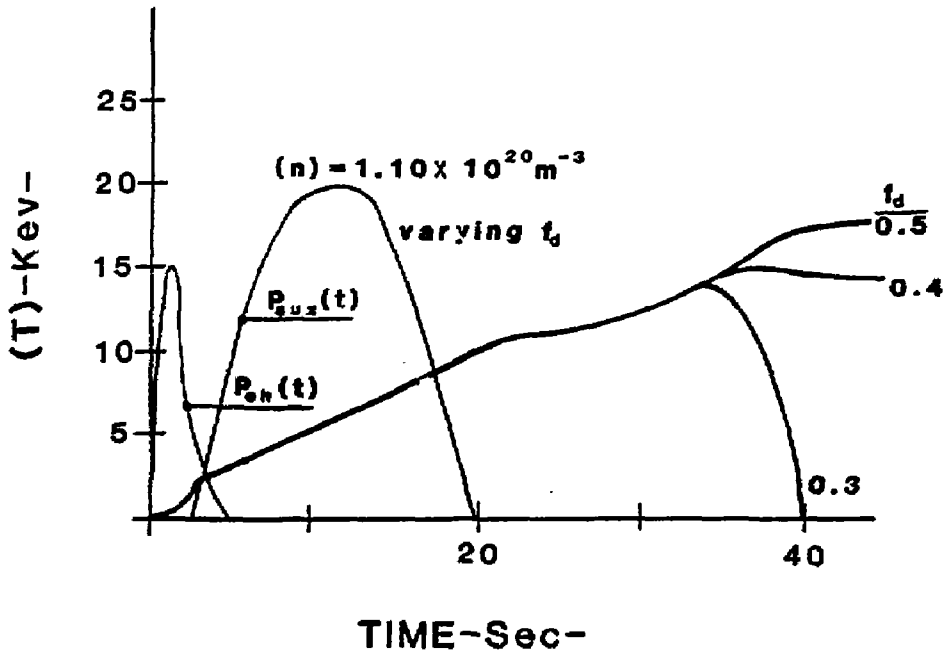
(T)-Kev-
25
20
15
10
5
(n) = 1.10 X 10^20 m^-3
varying t_d
P_aux(t)
P_oh(t)
t_d
0.5
0.4
0.3
20
40
TIME-Sec-

Figure 19

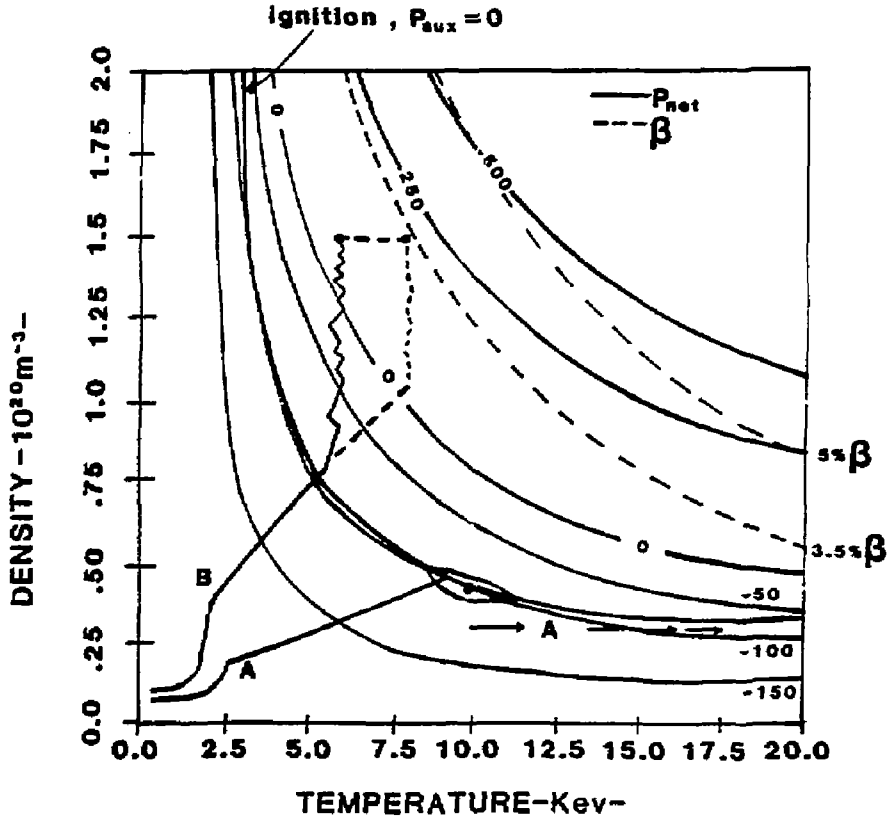
ignition , $P_{aux}=0$
P_{net}
β
DENSITY-$10^{20}m^{-3}$-
TEMPERATURE-Kev-
0.0 .25 .50 .75 1.0 1.25 1.5 1.75 2.0
0.0 2.5 5.0 7.5 10.0 12.5 15.0 17.5 20.0
0
250
500
5%β
3.5%β
-50
-100
-150
A
B

Figure 20

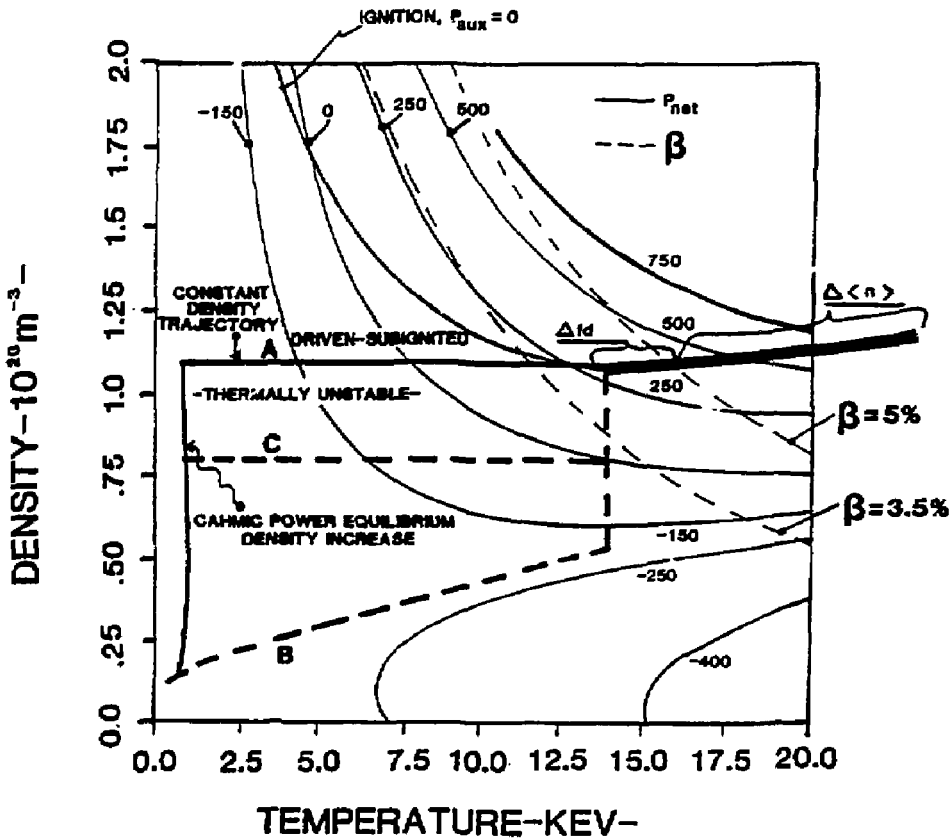
IGNITION, $P_{aux} = 0$
-150
0
250
500
P_{net}
β
750
500
250
$\Delta\langle n \rangle$
Δ id
CONSTANT DENSITY TRAJECTORY
A
DRIVEN-SUBIGNITED
-THERMALLY UNSTABLE-
C
OHMIC POWER EQUILIBRIUM DENSITY INCREASE
B
-150
-250
-400
β=5%
β=3.5%
DENSITY-10^{20} m^{-3}-
0.0 .25 .50 .75 1.0 1.25 1.5 1.75 2.0
0.0 2.5 5.0 7.5 10.0 12.5 15.0 17.5 20.0
TEMPERATURE-KEV-

Figure 21

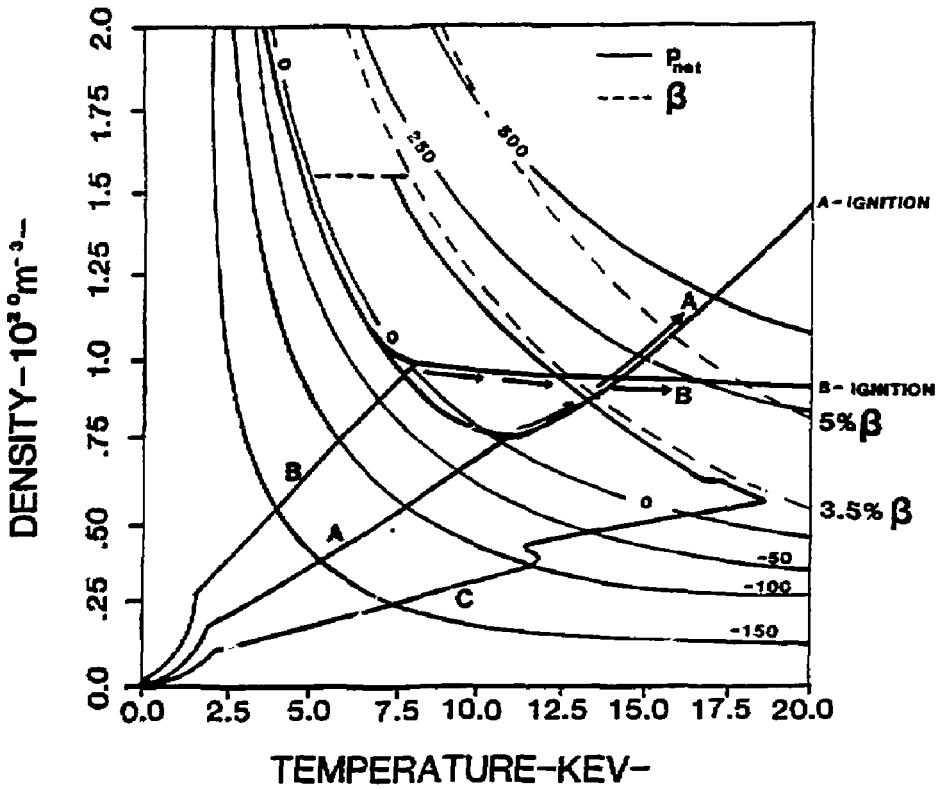
DENSITY-10^{20}m^{-3}-
TEMPERATURE-KEV-
0.0
.25
.50
.75
1.0
1.25
1.5
1.75
2.0
0.0
2.5
5.0
7.5
10.0
12.5
15.0
17.5
20.0
P_{net}
β
0
250
500
A- IGNITION
B- IGNITION
5%β
3.5%β
A
B
C
-50
-100
-150

Figure 22